Atmospheric Environment 237 (2020) 117674

Contents lists available at ScienceDirect

Atmospheric Environment

journal homepage: http://www.elsevier.com/locate/atmosenv

Contributions of traffic and shipping emissions to city-scale NO_x and $PM_{2.5}$ exposure in Hamburg

Martin Otto Paul Ramacher *, Volker Matthias, Armin Aulinger, Markus Quante, Johannes Bieser, Matthias Karl

Chemistry Transport Modelling Department, Institute of Coastal Research, Helmholtz-Zentrum Geesthacht, 21502, Geesthacht, Germany

HIGHLIGHTS

- We investigate the contribution of road traffic and shipping to $PM_{2.5}$ and NO_2 concentrations in the Hamburg urban area.
- Ship emissions are based on individual AIS position data and include emissions at berth, manoeuvring and cruising.
- Traffic contributes with 23% to NO_2 and 18% to $PM_{2.5}$ population weighted exposure.
- Shipping contributes with 14% to NO_2 and 3% to $PM_{2.5}$ population weighted exposure.
- On-shore electricity for ships at berth shows maximum reduction potentials of 35% for NO_2 and 30% for $PM_{2.5}$ for exposure.

ARTICLE INFO

Keywords:
Urban air pollution
Population exposure
NO_2
$PM_{2.5}$
Transport emissions
Road traffic
Shipping
Chemical transport modelling
TAPM

ABSTRACT

We investigated the contribution of road traffic and shipping related emissions of NO_2 and $PM_{2.5}$ to total air quality and annual mean population exposure in Hamburg 2012. For this purpose, we compiled a detailed emission inventory following SNAP categories focusing on the detailed representations of road traffic and shipping emissions. The emission inventory was applied to a global-to-local Chemistry Transport Model (CTM) system to simulate hourly NO_2 and $PM_{2.5}$ concentrations with a horizontal grid resolution of 500 m. To simulate urban-scale pollutant concentrations we used the coupled prognostic meteorological and chemistry transport model TAPM. The comparison of modelled to measured hourly values gives high correlation and small bias at urban and background stations but large underestimations of NO_2 and $PM_{2.5}$ at measurements stations near roads. Simulated contributions of road traffic emissions to annual mean concentrations of NO_2 and $PM_{2.5}$ is highest close to highways with relative contributions of 50% for NO_2 and 40% for $PM_{2.5}$. Nevertheless, the urban domain is widely affected by road traffic, especially in the city centre. Shipping impact focuses on the port and nearby industrial areas with contributions of up to 60% for NO_2 and 40% for $PM_{2.5}$. In residential areas in the north of the port, shipping contributes with up to 20–30% for NO_2 and $PM_{2.5}$. Our simulation resulted in 14% of the population of Hamburg being exposed to hourly NO_2 concentration above the hourly limit of 200 $\mu g/m^3$, <1% to annual NO_2 concentrations above the annual limit of 40 $\mu g/m^3$, and 39% to $PM_{2.5}$ concentrations above the annual WHO limit of 10 $\mu g/m^3$. The calculation of the population-weighted mean exposure (PWE) to NO_2 and $PM_{2.5}$ reveals mean exposures of 20.51 $\mu g/m^3$ for NO_2 and 9.42 $\mu g/m^3$ for $PM_{2.5}$. In terms of PWE to NO_2, traffic contributes 22.7% to the total and is 1.6 times higher than the contribution of shipping (13.9%). In total, traffic and shipping contribute with 36.6% to the NO_2 PWE in Hamburg in 2012. When it comes to $PM_{2.5}$, traffic contributes 18.1% and is 5.3 times higher than the contribution from shipping (3.4%). In total, traffic and shipping contribute 21.5% to the $PM_{2.5}$ PWE in Hamburg in 2012. Two local scenarios for emissions reductions have been applied. A scenario simulating decrease in shipping emissions by instalment of on-shore electricity for ships at berth, revealed reduction potentials of up to 40% for total NO_2 exposure and 35% for $PM_{2.5}$ respectively. A road traffic scenario simulating a change in the fleet composition in an inner city zone, shows lower reduction potentials of up to 18% for total exposure to NO_2 and 7% for $PM_{2.5}$ respectively. The discussion of uncertainties revealed high potentials for improving the emission inventories, chemical transport simulation setup and exposure estimates. Due to the use of exposure calculations for policy support and in health-effect studies, it is indispensable to reduce and quantify uncertainties in future studies.

* Corresponding author.
E-mail address: martin.ramacher@hzg.de (M.O.P. Ramacher).

https://doi.org/10.1016/j.atmosenv.2020.117674
Received 4 September 2019; Received in revised form 20 April 2020; Accepted 4 June 2020
Available online 16 June 2020

&alert_message_var;

1. Introduction

Today, urban air quality related issues are among the most critical societal concerns, because they affect the quality of life of a large and rapidly growing part of the world population: urban citizens. The large majority of Europeans living in urban environments are exposed to levels of air pollution considered dangerous for human health. According to the European Environment Agency (EEA), Europe's most serious atmospheric pollutants, which are harmful for human health, are particulate matter (PM_{10} and $PM_{2.5}$), nitrogen oxides (NO_x) and ground-level ozone (O_3) (WHO, 2006). Between 2014 and 2016, 6–8% of the European Union (EU-28) urban population was exposed to $PM_{2.5}$ levels above the EU limit of 25 μg m^{-3}, while 7–8% of the EU-28 urban population were exposed to nitrogen dioxide (NO_2) concentrations above the EU annual limit of 40 μg m^{-3} (Guerreiro et al., 2018). Considering the WHO reference concentrations of 10 μg m^{-3} for $PM_{2.5}$, 74–85% of the urban EU-28 population have been exposed to $PM_{2.5}$ levels above the limits.

Exposure to air pollution can lead to asthma, respiratory and cardiovascular diseases, lung cancer and premature deaths (WHO, 2006). Several studies prove a causal relation of human exposure to emissions and ambient concentrations of pollutants as particulate matter (PM_x) nitrogen oxides (NO_2 and nitric oxide, NO) in urban areas and for short- and long-term health effects (Hoek et al., 2013; WHO, 2016a). While exposure to $PM_{2.5}$ was estimated to be a leading cause of the environmental burden of disease in six selected European countries (Hänninen et al., 2014), the relationship between NO_2 and health is scientifically not as well founded as for $PM_{2.5}$ (WHO, 2006; Heroux et al., 2013). However, NO_2 is usually regarded as an indicator of other pollutants and long-term residential exposure to NO_x is moving into focus due to rising evidence for severe health-effects of the respiratory system (Hamra et al., 2015; WHO, 2016b; Wing et al., 2018), and as risk factor for myocardial infarction (Rasche et al., 2018). This emphasizes the need for emission reduction in sectors contributing to NO_x and $PM_{2.5}$ emissions.

The transport sector is one of the most challenging areas, when it comes to abatement of local air pollution. NO_x, volatile organic compounds (VOC), carbon monoxide (CO) and PM_x emissions as well as precursors for secondary organic aerosols (SOA), from the transport sector account for a significant share of the global and regional greenhouse gas and air pollutant burden (Unger et al., 2008; Uherek et al., 2010; Kiesewetter and Amann, 2014; Carslaw et al., 2016, 2019). Currently, transport by means of road, rail, water and air remains largely fossil fuel driven and represents a major contribution to global climate gases and air pollutants. This directly affects the health of millions of people especially in larger cities and agglomeration areas. When it comes to NO_x emissions, transport was the main contributor to total emission sources in the EU in 2016, divided into 39% for road transport and 9% for non-road transport, including shipping activities. Regarding $PM_{2.5}$, the contributions are 11% for road transport and 2% for non-road transport (Guerreiro et al., 2018). Ambient $PM_{2.5}$ is composed of a variety of components, originating from local emissions as well as transboundary transport of pollution from natural as well as anthropogenic activities of many economic sectors. While primary PM_x is mainly emitted from traffic and household combustion, secondary PM in Europe is predominantly formed from precursor emissions from agriculture, industrial and traffic sources (Kiesewetter and Amann, 2014; Backes et al., 2016). In terms of urban background $PM_{2.5}$, it has been shown that in southern Europe 65–70% of the concentration arises from secondary aerosols, whereas only 30–35% is attributed to primary aerosols (Amato et al., 2016). This reinforces the fact that both PM gaseous precursors and primary PM should be abated to reduce PM pollution. In terms of health effects due to traffic emissions, Künzli et al. (2000) estimated the impact of outdoor (total) and traffic-related air pollution on public health in Austria, France, and Switzerland and found out that air pollution caused 6% of total mortality or more than 40,000 attributable cases per year, while about half of all mortality caused by air pollution was attributed to motorised traffic. Moreover, Nawrot et al. (2011) identified exposure to road traffic as the single biggest population-attributable risk factor for triggering acute myocardial infarction. Although there are recent studies that show e.g. evidence that the proportion of NO_x emitted as NO_2 has levelled-off or decreased at roadside measurement sites (Carslaw et al., 2016; Grange et al., 2017), road transport was still Europe's biggest single source for NO_x and the second biggest for $PM_{2.5}$ in 2016 (Guerreiro et al., 2018). Thus, transport activity across Europe is high, and set to continue growing – estimates suggest that passenger transport will increase by 42% by 2050, and freight transport by 60% (European Commission, 2019).

The average contribution of shipping emissions to the population exposure from primary $PM_{2.5}$, NO_x, and SO_x is 8%, 16.5%, and 11%, respectively, across Europe (Andersson et al., 2009). Corbett et al. (2007) stated that shipping-related PM emissions are responsible for approximately 60,000 cardiopulmonary and lung cancer deaths annually, with most deaths occurring in coastal regions of Europe, East Asia, and South Asia. An update of this study shows that despite implemented regulations, low-sulphur marine fuels will account for 250,000 deaths annually in 2020 due to a projected increase in transport by sea (Sofiev et al., 2018). Thus, transport activities, such as road traffic and shipping are of major interest for policy actions to improve urban air quality and urban citizen's health, especially in harbour cities.

To support policy actions and identify impacts of planned regulations, information about the spatial distribution of emissions and their sources, as well as the resulting concentration and exposure to health related pollutants are necessary. This information can be provided by city scale Chemistry Transport Model (CTM) systems, which are an indispensable tool to assess the current and future air quality and to support Air Quality Management (AQM). In addition, CTM systems enable the contribution of specific emission sources and sectors to spatially resolved concentrations and exposure to be identified.

This study investigates the contribution of local road traffic and shipping emissions to $PM_{2.5}$ and NO_2 concentrations in the harbour city of Hamburg in 2012. The Free and Hanseatic City of Hamburg is a federal state and the second-largest city in Germany with a population of over 1.8 million people. Hamburg lies along the River Elbe, which connects the city with the 110 km distant North Sea, making it the gateway to Europe's third largest international port: the Port of Hamburg. The Port of Hamburg was and is the most significant economic sector in Hamburg and is additionally one of Hamburg's largest tourist attractions. Nevertheless, activities attributable to the Port of Hamburg, such as shipping and freight traffic, are affecting the cities' air quality. According to the municipality of Hamburg, road traffic and shipping have been contributing 35% and 38% to total NO_x emissions and 30% and 17% to total PM_{10} emissions in 2012, making the transportation sector the largest emission source for NO_x and PM_{10} (Böhm and Wahler, 2012). Although overall air quality in Hamburg has improved in recent decades, there are still exceedances of NO_2 limits as defined by air quality standards of the European Union. In Hamburg there is a well-established air quality monitoring network (Hamburger Luftmessnetz, HaLM, http://www.luft.hamburg.de) continuously measuring air pollutants such as NO_2, NO, PM_{10}, $PM_{2.5}$, sulphur dioxide (SO_2), CO, O_3 and several heavy metals. It consists of about 15 measurement stations, both at traffic and urban background sites. The aim of the monitoring network is to observe long-term trends and to detect possible exceedances of limits. Because PM_{10} and NO_2 limits were exceeded in recent years, especially at traffic stations, the municipality of Hamburg established its first Clean Air Plan to tackle these

exceedances with a variety of actions in 2004 (Behörde für Stadtentwicklung und Umwelt, 2004). The Clean Air Plan was updated in 2012 due to ongoing exceedances of annual limits of PM_{10} as well as of annual and hourly limits of NO_2 (Böhm and Wahler, 2012). A second update of the Clean Air Plan for Hamburg in 2017 identified annual limit exceedances for NO_2 at near-road stations, while measured PM_{10} concentrations are now below EU limits (Behörde für Umwelt und Energie, 2017). Following the WHO guidelines for air quality limits, there is even more need for improving the air quality in Hamburg to reduce the impact of air pollution on public health. Therefore, it is necessary, to identify major sources of emissions and to understand the chemical conversion and spatial distribution of the different compounds in the urban atmosphere. Moreover, possible impacts of different emission reduction scenarios should be investigated in scenario simulations, to design effective measures for combating air pollution and supporting policy efforts in tackling questions of air quality management.

To identify the atmospheric transport and chemical transformation of emissions from traffic and shipping, we compiled a detailed emission inventory for all sectors in high spatio-temporal resolution for the year 2012 in the metropolitan area of Hamburg. We used this emission inventory in an urban-scale CTM system to model the total annual concentration of NO_2 and $PM_{2.5}$, the contribution of road transport emissions and the contribution of local shipping emissions to the total concentrations. Additionally, we created local emission reduction scenarios for road traffic and shipping activities and applied these scenarios in the CTM system. We decided to model $PM_{2.5}$ emissions instead of PM_{10} emissions, due to its better-established impact on human-health impact through epidemiological studies. For quality assurance, we compared hourly-modelled concentrations with measurements from the Hamburg air quality observation network. Additionally, we identified the contribution of traffic and shipping for all locations of the observational network. Based on evaluated surface concentration fields we calculated the annual mean population exposure in Hamburg to road transport emissions and to shipping emissions as well as for two local emission reduction scenarios using high-resolution population counts at residential addresses. The calculated concentration and exposure maps enable the identification of hotspots and reduction potentials due to different emission reductions scenarios, which are valuable information for supporting urban air quality management strategies as well as health effect studies in Hamburg.

This study demonstrates that with an established model and carefully compiled emission data a thorough air quality study on the urban-scale can be accomplished, allowing for spatial analyses of sectoral contributions to pollutant concentrations and related exposure of city dwellers. Furthermore, the setting was used to explore the emission reduction potential of certain scenarios currently under political discussion or suggested by the actors of the civil society. Although being a study conducted for a selected town, the evaluated procedure can be certainly transferred to other cities or localized emission hot spots.

In section 2, we describe the urban-scale Chemistry Transport and Exposure Model setup including a detailed description of the high-resolution emissions inventory compilation and the development of different local emissions scenarios for Hamburg. The modelled concentrations of NO_2 and $PM_{2.5}$ are evaluated in section 3.1, and the results for total surface concentrations as well as the contributions of road transport and shipping are presented in section 3.2. The annual mean population exposure to NO_2 and $PM_{2.5}$ is presented in section 3.3. Section 3.4 displays results of the simulated local emission reduction scenarios, which is followed by an extensive discussion of uncertainties in section 4 and conclusions in section 5.

2. CTM & exposure simulation setup

We used an offline coupled urban-scale meteorology and chemistry transport modelling system (see Fig. 1) to simulate concentrations of and population exposure to $PM_{2.5}$ and NO_2 in Hamburg for the year 2012.

2.1. CTM setup

To model local scale hourly surface concentration of NO_x and $PM_{2.5}$ we used the coupled meteorological and Chemistry Transport Model TAPM (Hurley et al., 2005; Hurley, 2008). TAPM has both a meteorological component and an air quality component and has been applied and validated over several European regions showing good performance in the prediction of air pollutant concentrations (e.g. Ambrey et al. (2014), Duque et al. (2016), Fridell et al. (2014), Gallego et al. (2016), Rafael et al. (2015) or Matthaios et al., 2018). The meteorological component of TAPM is an incompressible, non-hydrostatic, primitive equation model with a terrain-following vertical sigma coordinate for 3-D simulations. The model solves the momentum equations for horizontal wind components, the incompressible continuity equation for vertical velocity, and scalar equations for potential virtual temperature and specific humidity, cloud water/ice, rain water and snow (Hurley, 2008). Using predicted meteorology and turbulence from the meteorological component, the air pollution component solves prognostic equations for concentrations and cross-correlation of concentrations using an Eulerian grid module. The Eulerian Grid Module (EGM) consists of nested grid-based solutions of the Eulerian concentration mean and optionally variance equations representing advection, diffusion, chemical reactions and emissions. It includes gas-phase photochemistry based on the Generic Reaction Set (GRS) of Azzi et al. (1984), gas- and aqueous-phase chemical reactions for SO_2 and PM based on Seinfeld and Pandis (1998), formation of ozone from NO_x and VOCs and a simple parametrization of the formation of secondary organic aerosol. In TAPM, formation of VOC is treated as VOC reactivity (RSmog). The concept of using VOC reactivity rather than VOCs in the reaction equations follows from the work of Johnson (1984). The concentration of Rsmog is defined as a reactivity coefficient multiplied by VOC concentration. In this study, we used a VOC reactivity value of 0.0067, which is then multiplied with the annual VOC emissions of all sources to account for VOCs in chemical reaction in the TAPM air pollution component. This value follows the work of Johnson (1984) and represents Australian urban air conditions, which are dominated by motor vehicles. The model also treats dry and wet deposition processes of gases and PM as well as the secondary formation of PM_{10} and $PM_{2.5}$. A range of pollutant emission configurations can be used, including point sources, line sources, area/volume sources and gridded surface sources.

In this study, we setup the air pollution component of TAPM with a horizontal rectangular grid resolution of 500 m and an extent of 28×28 km^2, covering the entire urban core area of Hamburg, as well as suburban and some rural parts of the metropolitan area of Hamburg (Fig. 2a). The vertical layer structure of meteorological and pollution simulations with TAPM was 30 layers with a layer top at 8000 m height above ground. The layer top heights of the lowest 10 layers were: 10 m, 25 m, 50 m, 75 m, 100 m, 150 m, 200 m, 250 m, 300 m, and 350 m. Table 1 provides details of the vertical and horizontal configuration of TAPM for the meteorological and pollution grid.

The air pollution component of TAPM is off-line coupled to the inner meteorological domain D4 as well as background concentration fields to account for initial and boundary conditions of chemical compounds. Thus, TAPM was set-up as part of a one-way nested model chain, which coupled the model off-line to the CMAQv5.0.1 CTM (Byun and Schere, 2006) driven by COSMO-CLM mesoscale meteorological model version 5.0 (Rockel et al., 2008) for the year 2012 using the ERA-Interim re-analysis as forcing data. Hourly concentrations are used at the boundaries to account for background concentrations in the CTM domain. Since TAPM allows only 1-d boundary concentration fields with time being the only variable, the TAPM boundary concentrations were calculated using the horizontal wind components on each of the four lateral boundaries for weighting the boundary concentrations around the TAPM model domain (Tang et al., 2020).

We used all relevant emission sources (see section 2.3) in the pollution component and ran TAPM simulations with the described

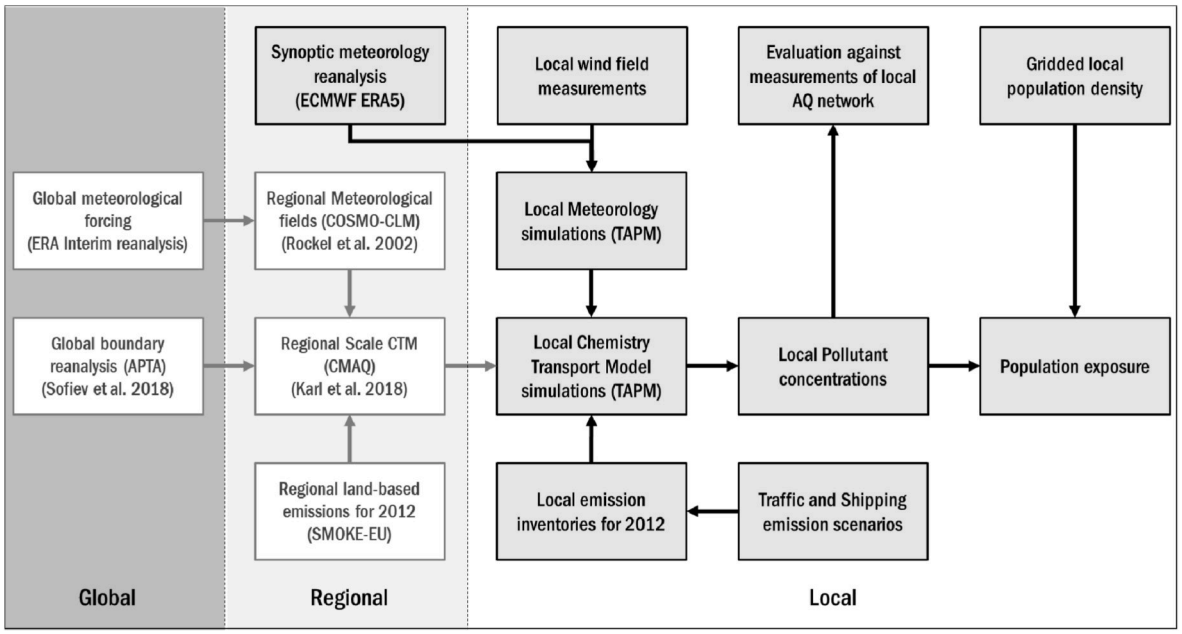

Fig. 1. Study Design to derive population exposure to NO_2 and $PM_{2.5}$ concentrations in Hamburg 2012. Boxes shown greyed out represent global and regional data from other studies, which were used in this study to drive the local-scale simulations.

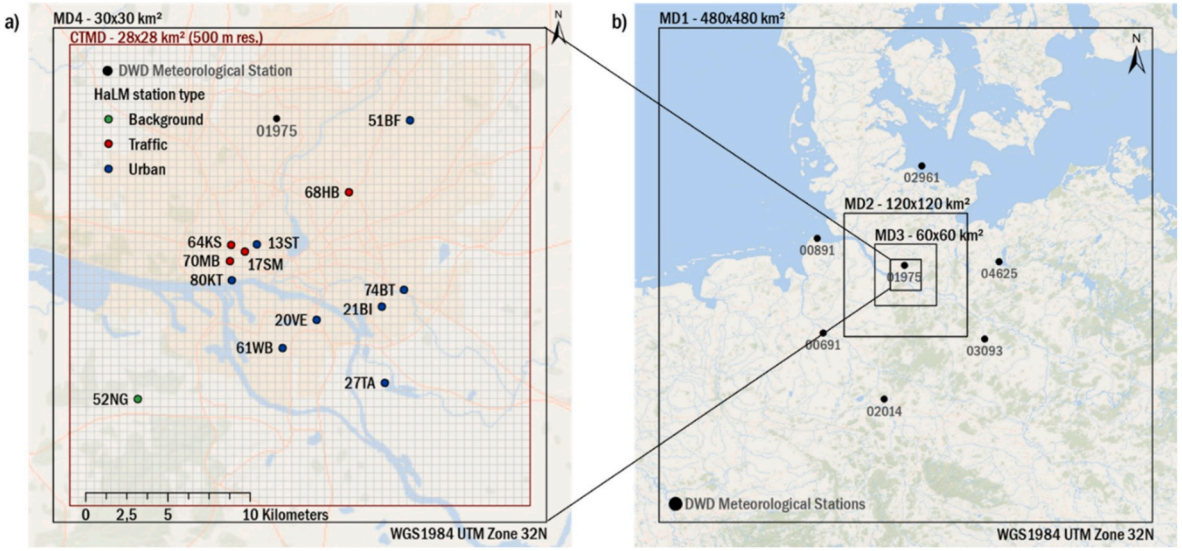

Fig. 2. Urban-scale simulations with the TAPM Air Pollution component in domain CTMD, which is nested in the meteorological domain MD4 (a). Nested meteorological simulations with TAPM driven by ERA5 synoptic reanalyses ensemble means (b).

settings for year 2012 to calculate hourly concentrations of NO_x, NO_2, O_3, SO_2, PM_{10} and $PM_{2.5}$ (base scenario). To identify the impact of shipping and traffic emissions we used the zero-out method and thus, ran additional simulations without shipping emissions (no_ship) and without traffic emissions (no_traffic). We evaluated the simulated base scenario concentrations with all available observations in the TAPM domain (see section 3) and analysed the results of all scenarios in terms of source contributions. Basic model settings are listed in Table 1.

2.2. Meteorology setup and evaluation

TAPM includes a nested approach for meteorology, which allows a user to zoom-in to a local region of interest quite rapidly, while the outer boundaries of the grid are driven by synoptic-scale analyses. We applied the meteorological component with four nested domains from 480 × 480 km^2 extent to 30 × 30 km^2 extent (Fig. 2b). The outer domain (D1) is driven by three-hourly ECMWF ERA5 synoptic scale reanalyses ensemble means on a longitude/latitude grid with 0.3 × 0.3° resolution and a vertical structure following the vertical structure of the TAPM setup (Table 1). In all meteorological simulations, a vegetative canopy scheme, soil scheme, and an urban scheme with 7 urban land use classes (Hurley, 2008) are used at the surface, while radiative fluxes, both at the surface and at upper levels, are also included. Terrain elevation data was adopted from the German Digital Elevation Model (EEA, 2017) at 200 m horizontal resolution and the land use information was adopted from the CORINE Land Cover 2012 database (Copernicus Land Monitoring Service, 2018) at 100 m horizontal resolution. Moreover, we assimilated hourly measurements of seven meteorological stations (Fig. 2b) to nudge simulations in TAPM. This meteorological setup for Hamburg in 2012 was applied and evaluated in a study by Karl et al. (2019), which used

Table 1
Horizontal and Vertical Structure of Meteorological and Air Pollution simulations with TAPM.

	Meteorological Module	Air Pollution Module
Horizontal Size of the Domains (X,Y)	MD1: 480 × 480 km^2 MD2: 120 × 120 km^2 MD3: 60 × 60 km^2 MD4: 30 × 30 km^2	CTMD: 28 × 28 km^2
Horizontal Resolution	MD1: 16000 m MD2: 4000 m MD3: 2000 m MD4: 1000 m	CTMD: 500 m
Model grid and coordinate system	Universal Transverse Mercator (UTM) with WGS 1984 as reference geoid, Zone 32N	
Dec. Deg. grid Centre coordinates [lat, lon]	53.54755, 10.00744	
UTM grid centre coordinates [m]	566750, 5933656	
Vertical dimension and coordinate	30 layers, terrain-following sigma-coordinate system	
Vertical layers top heights [m]	10, 25, 50, 75, 100, 150, 200, 250, 300, 350, 400, 450, 500, 600, 750, 1000, 1250, 1500, 1750, 2000, 2250, 2500, 3000, 3500, 4000, 4500, 5000, 6000, 7000, 8000	

the meteorological output fields of TAPM to drive the urban-scale CTM EPISODE-CityChem, as well as for CTM simulations with TAPM with a horizontal resolution of 1000 m. Furthermore, the meteorological performance of TAPM has been evaluated in Karl et al. (2019) and showed good agreement with observed values at different sites and in different heights for temperature, radiation, wind speed and wind direction.

2.3. Reference emissions for the year 2012

Reliable emission data are probably the most important input for chemistry transport model (CTM) systems (Matthias et al., 2018; Bieser et al., 2020) and have been identified as a major area for improvements during previous model studies in local-scale simulations for the city of Hamburg (Ramacher et al., 2018). Therefore, we compiled a detailed emission inventory for NO_x, CO, NMVOC, SO_2, PM_{10} and $PM_{2.5}$ from various data sources to capture major emission sources following SNAP (Selected Nomenclature for Air Pollution) emission sectors. We divided the emission inventory into area, line and point sources to account for the spatial characteristics of different emission sources. Table 2 lists the necessary information. This emissions inventory for Hamburg 2012 was compiled and applied by Karl et al. (2019) and is a refinement of an inventory used in a previous study on the urban air quality in Hamburg (Ramacher et al., 2018). The temporal disaggregation by sector for each source type was done with the Urban Emission Conversion Tool (UECT, Hamer et al., 2019). UECT is a utility for preparing emission input files with hourly emission values for NO_x, NMVOC, CO, SO_2, NH_3, $PM_{2.5}$ and PM_{10} based on the yearly emissions for the city being studied. The UECT converts annual emission totals to hourly emissions using SNAP sector specific profiles (Denier Van Der Gon et al., 2011; Hamer et al., 2019). The results are formatted into emission input files for TAPM and contain hourly varying emission data for each source category and pollutant.

Large emission sources from combustion and industrial processes (SNAP 1, 4, 5, 9) are modelled as point sources and were collected from the registry of emission data in Hamburg as reported under the German Federal Immission Control Act (BImSchV 11). We combined this data with a data set on European stack characteristics by Pregger and Friedrich (2009) to account for stack heights, exit temperature and exit velocities for plume rise calculations in TAPM.

For area sources, we mainly used spatially gridded annual emission totals with a grid resolution of 1 × 1 km^2 provided by the German Federal Environmental Agency (Schneider et al., 2016) for 2012. The spatial distribution of the annual emission totals for our research area has been done at UBA using the ArcGIS based software GRETA

Table 2
Emission sectors data for the simulation of air quality in Hamburg following the SNAP classification.

SNAP	SNAP name	Source type	Vertical distribution	Emission data source
01	Combustion in energy and transformation industries	Point	Plume rise	Reported under the German Federal Emission Control Act. Combined with dataset on European stacks (Pregger and Friedrich, 2009)
02	Non-industrial combustion plants (domestic heating)	Area (1 × 1 km^2)	First layer (10 m)	Umweltbundesamt emission inventory, GRETA software (Schneider et al., 2016)
03	Combustion in manufacturing industry	Area (1 × 1 km^2)	First layer (10 m)	Umweltbundesamt emission inventory, GRETA software (Schneider et al., 2016)
04	Production processes	Point	Plume rise	Reported under the German Federal Emission Control Act. Combined with dataset on European stacks (Pregger and Friedrich, 2009)
05	Extraction and distribution of fossil fuels and geothermal energy	Point	Plume rise	Reported under the German Federal Emission Control Act. Combined with dataset on European stacks (Pregger and Friedrich, 2009)
06	Solvent and other product use	Area (1 × 1 km^2)	First layer (10 m)	Umweltbundesamt emission inventory, GRETA software (Schneider et al., 2016)
07	Road transport	Line	0 m above ground	Hamburg municipality inventory (Lorentz et al., 2010), emission factors from HBEFA version 3.1 (UBA, 2010)
08	Other mobile sources and machinery (without shipping)	Area (1 × 1 km^2)	First layer (10 m)	Umweltbundesamt emission inventory, GRETA software (Schneider et al., 2016)
0804	Shipping	Area (1 × 1 km^2)	First layer (10 m)	Aulinger et al. (2016)
09	Waste collection, treatment and disposal activities	Point	Plume rise	Reported under the German Federal Emission Control Act. Combined with dataset on European stacks (Pregger and Friedrich, 2009)
10	Agriculture and farming	Area (1 × 1 km^2)	First layer (10 m)	Umweltbundesamt emission inventory, GRETA software (Schneider et al., 2016)

("Gridding Emission Tool for ArcGIS"), which can generate emission data sets for all SNAP sectors for Germany (Schneider et al., 2016). From this dataset annual emission totals with 1-km horizontal resolution for the SNAP categories 02 (domestic heating), 03 (commercial combustion), 06 (solvent and other product use), 08 (other mobile sources, excluding shipping), and 10 (agriculture and farming) were derived. We temporally disaggregated these annual totals using sector-specific monthly, weekly and hourly profiles (Denier Van Der Gon et al., 2011). For SNAP 2 (domestic heating) we additionally used the daily averaged ground air temperature obtained from the first layer (0–10 m) of the meteorological TAPM simulation to create annual temporal profiles. Day-to-day variation of domestic heating emissions is based on the heating degree day concept, implemented in the UECT (Hamer et al.,

2019).

Besides these SNAP sectors, we also considered shipping as an area source. The gridded ship emission inventory (SNAP0804) for the port area of Hamburg was created in a bottom-up approach. This approach uses Automatic Identification System (AIS) data, which tracks individual ship movements and estimates engine loads from the ship's speed over ground, provided the maximum continuous rating (MCR) – the power corresponding to the maximum speed is available. In case the engine characteristics of a specific ship are missing, median characteristics of the respective size class are used. This data was combined with activity based emission factors for NO_x, SO_2, CO, CO_2, hydrocarbons (VOC), and PM to calculate local shipping emissions while sailing (Aulinger et al., 2016). Emissions of ships manoeuvring and hoteling were calculated from an estimated fuel consumption according to Hulskotte and Denier Van Der Gon (2010). The calculated shipping emission totals were spatially distributed on a 250 m × 250 m grid according to the ship routes inside the port area. A temporal resolution of 1 h was achieved using ship-specific activity data derived from hourly AIS positioning data.

The road traffic emission inventory is based on 15,816 line source segments each providing emissions of NO_x, NO_2, PM_{10} and $PM_{2.5}$ for the entire Hamburg road network. The data were provided by the city of Hamburg and calculated using a bottom-up approach with emission factors from HBEFA version 3.1 and based upon traffic densities and fleet compositions measured, calculated or estimated for per road segment (Lorentz et al., 2010). The NO_x emission factor from road traffic for the year 2012 was increased by 20% for all street types because the average NO_x emission factor in the new HBEFAv3.3 for passenger cars is higher by 19.4% (diesel cars: 21%) than in HBEFAv3.1 used in the road emission inventory (UBA, 2010). To estimate NMVOC traffic emissions, an average NMVOC/NO_x ratio of 0.588, derived from UBA data for SNAP cat. 07, was used. A NO_2/NO_x ratio of 0.3 was applied to re-calculate NO_2 emissions for this study because of the expected higher real-world NO_2 emissions from diesel vehicles. Considerations based on the higher NO_2/NO_x ratio from diesel passenger cars (from 0.12 to > 0.5; Carslaw and Rhys-Tyler, 2013) and the review by Kurtenbach et al. (2012) who assumed that Euro 4–6 passenger cars emit 55% of the total NO_x as NO_2, justify the use of the high NO_2/NO_x ratio for the Hamburg vehicle fleet.

In the road traffic emission inventory PM_{10} and $PM_{2.5}$ emissions are given as total emissions including exhaust emissions (tailpipe) and non-exhaust (non-tailpipe) traffic related particles such as brake, tyre, clutch and road surface wear or already deposited particles in the environment, which become re-suspended due to traffic induced turbulence (Lorentz et al., 2010). Nevertheless, first attempts to apply the road traffic emission inventory led to high underestimations of PM_{10} and $PM_{2.5}$. A literature review by Grigoratos and Martini (2014) estimate that brake, tyre and road wear along with road dust resuspension are the most important non-exhaust traffic related sources for PM, with their relative contributions to non-exhaust traffic related emissions ranging between 16 and 55% (brake wear), 5–30% (tyre wear) and 28–59% (road dust resuspension). Moreover, braking was identified to be a major source of non-exhaust traffic-related emissions particularly in urban locations (Grigoratos and Martini, 2014). Thus, we decided to double the total road traffic emissions for PM_{10} and $PM_{2.5}$ as given by Lorentz et al. (2010), to consider non-exhaust emissions sufficiently and balance the unavailable information on non-exhaust fraction in total emissions. Additionally, we altered the PM_{10} and $PM_{2.5}$ emissions, to account for secondary organic aerosol (SOA) emissions, which is formed by condensation and oxidation of VOCs in hot exhaust emissions depending on surrounding atmospheric conditions and types of exhausted VOCs. For example in the case of wood combustion emissions, van der Denier Gon et al. (2015) argued that emission factors are used that are obtained from measurements in hot air directly after emission, while condensation may occur immediately when the emitted air is cooled down to ambient conditions, increasing the effective emissions. Moreover, SOA formation is a process expected to be important in the near roadway environment for traffic emissions (Pierce et al., 2009; Pirjola et al., 2015) but probably not accounted for in most emission inventories (Hendriks et al., 2013). Nevertheless, condensation and evaporation of organic vapors emitted from road traffic happens on small-scales (Zhang et al., 2004), which are not represented in urban dispersion modelling. Thus, we doubled the reported PM_{10} and $PM_{2.5}$ exhaust emissions, to account for missing particles from SOA formation and to account for underestimations in first modelling attempts. In total, the reported traffic emissions PM_{10} and $PM_{2.5}$ road traffic emissions were altered with a factor of three, to achieve results comparable with measurements.

The compiled emission inventory for Hamburg in 2012 comprises 17.9 kt NO_x and 2.5 kt $PM_{2.5}$ (Fig. 3). Emission inventories, which were used by the Hamburg municipality for air quality reporting (Böhm and Wahler, 2012), comprise 20.1 kt NO_x and 2.5 kt PM_{10} but no information on $PM_{2.5}$ was available. Thus, we compared modelled NO_x and PM_{10} emissions with reported NO_x, and PM_{10} emissions. NO_x emission sources are by 10% lower in our compiled emission inventory. When it comes to sectoral contributions road transport and shipping with 38.5% and 27.4% were identified as main contributors to NO_x emissions (Fig. 3a), while other sectors merely reach 10%. Comparing this to municipality reports with a contribution of 35% NO_x from traffic and 38% NO_x from shipping, the compiled inventory matches well with traffic contributions but have 10 percentage points lower contribution from shipping. While a sophisticated bottom-up approach for modelling shipping emissions was used, using positioning data and ship characteristics and included hoteling emissions, the shipping emissions in the Hamburg air quality report are adjusted for hoteling. In terms of PM_{10}, modelled emissions are 1.9 times higher than reported. This is mainly due to the introduced adjustment of traffic emissions. While in the reported emissions inventory PM_{10} from traffic accounts for 30% with 761 t, we applied PM_{10} traffic emissions of 2602 t and a relative contribution of 55%. Shipping was reported with 420 t (17%) of PM_{10}, which is fairly well captured by our calculations for shipping emissions with 380 t (3.3%). Taking into account our alteration of PM emissions, the compiled PM_{10} emissions achieve good agreements with the reported emissions inventory and we expect a similar quality for modelled $PM_{2.5}$ emissions. $PM_{2.5}$ (Fig. 3b) from road transport is dominating the local emission sources with 64.7% contribution, while shipping contributes with 6.4%. Thus, industrial emissions are the second-most important contributor to $PM_{2.5}$ emissions.

2.4. Traffic and shipping emission reduction scenarios

We created two different emission reduction scenarios to identify the impact of suitable local emission reduction actions for road traffic and shipping activities in the city of Hamburg. An actual implementation of both scenarios will certainly take a few years; however, if immediate actions are taken they could be in place in 2030. The first scenario focusing on shipping activities is based on the implementation of on-shore electricity for ships at berth and is called "land-powered ships" scenario. The second scenario focusing on road traffic is based on a changed car fleet composition in the inner city of Hamburg and is called "inner city zone" scenario. An overview of calculated emission reductions can be found in Table C1.

In the "land-powered ships" scenario, all emissions from ships at berth are assumed to be avoided due to extensive use of on-shore electricity for activities at berth. Several studies have shown that the emissions from ships at berth are a major contributor to emissions from shipping activities in ports (e.g. Hulskotte and Denier Van Der Gon, 2010; Corbett and Koehler, 2003; Liu et al., 2017) and that an implementation of on-shore electricity can bring substantial air quality improvements (e.g. Kotrikla et al., 2017; Chen et al., 2019; Ramacher et al., 2020). In Hamburg, the port area is located closely to densely populated areas in the east and north of the harbour area and thus, it can be expected that a reduction in emissions from shipping activities at berth will have an impact on population exposure to pollutants. Schnabel and

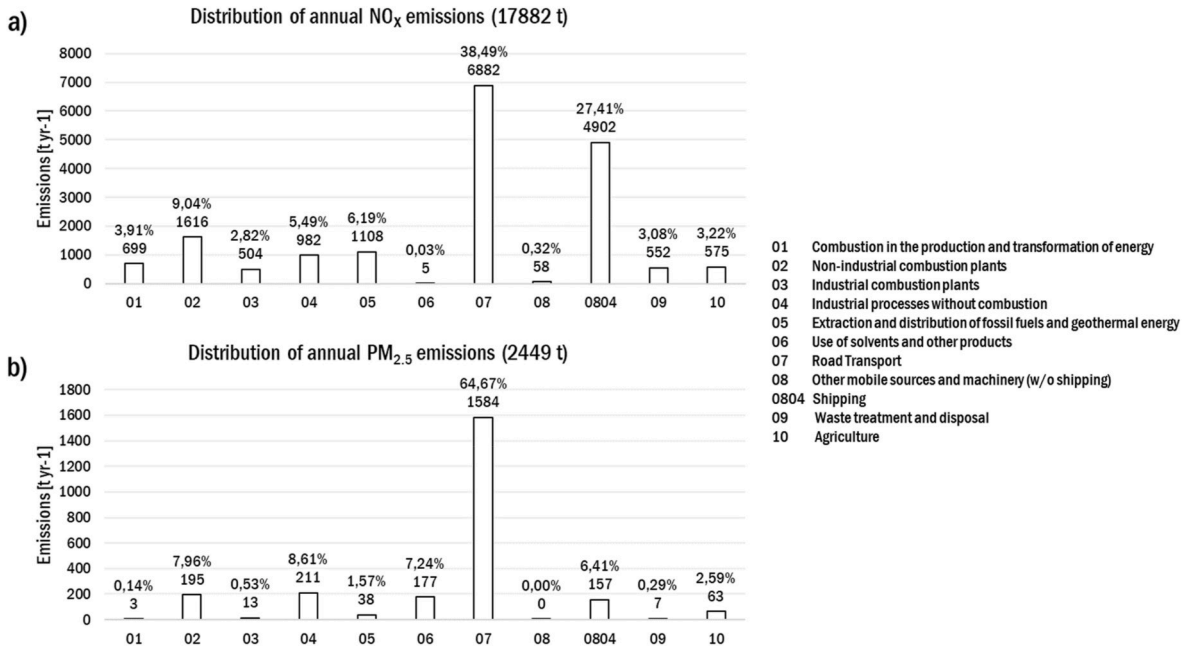

Fig. 3. Distribution of annual NO_x as NO_2 (a) and $PM_{2.5}$ (b) emissions in Hamburg 2012) by SNAP sector.

Beiersdorf (2018) have already discussed the technical opportunities for at least partial installation of on-shore electricity for ships at berth in the port of Hamburg. In this study, we applied a method for calculating ship emissions by Aulinger et al. (2016) which takes into account emissions from ships at berth (section 2.3), based on the ships berthing locations and emissions factors specific for berthing activities. Thus, in the "land-powered ships" scenario we excluded the hoteling emissions from the ship emissions inventory and kept only emissions for maneuvering and cruising in the port area. Thus, this scenario offers the opportunity to gather insights for a maximum reduction potential due to installation and usage of on-shore electricity for ships at berth. The calculated emission reductions are 1830 t NO_x and 70 t $PM_{2.5}$, which are 37% less NO_x and 45% less $PM_{2.5}$ emissions from shipping in the reference scenario. Thus, in the "land-powered ships" scenario shipping still contributes with 3072 t NO_x (17.2%) and 87 t PM2.5 (3.6%) to the total emissions in 2012.

In the "inner city zone" scenario, the car fleet composition was changed to an environmentally desirable but realistic fleet composition. Hamburg was the first city in Europe, in which diesel driving bans for single streets came into force in 2018. Moreover, an inner city zone for regulating access of vehicles of specific emission standards (Lorentz et al., 2010) was discussed in the past and is regularly topic of public and politic debates. Thus, we created a scenario, which describes an environmentally desirable fleet composition in an inner city-zone in Hamburg. We adapted emissions reductions for a fleet composition from a reference scenario for Germany in 2040 (Matthias et al., 2020; Seum et al., 2020). The adopted scenario comprises of 16.6% cars with EURO-6 emission standard, 61% hybrid electric vehicles with EURO-6 emission standards, 22% plug-in hybrid electric vehicles, and battery electric vehicles. The underlying reference scenario (Ehrenberger et al., 2020) represents a continuation of currently existing trends, but also moderate improvements regarding the implementation of new technologies and the use of renewable energies in the transport sector. Thus, the scenario describes a fleet composition, which is about to become reality in the next 20 years, considering current trends and projections. In our study, we chose the fleet mix for 2040 described in Matthias et al. (2020) and applied it to an inner city zone in Hamburg. Practical implementations of "green" or "blue" city zones, which are regulating access for cars with certain emission standards, have been applied in several German cities. Nevertheless, by also taking into account a substantial amount of electric cars, we aim at the environmentally best possible fleet composition, to show maximum reasonable reduction potentials for an inner city zone. Although the scenarios are for 2040, emissions in city zones will decrease earlier because of stricter regulations. The savings in emissions are derived from Matthias et al. (2020), who compared emissions in 2010 with their future reference scenario in 2040. The derived reduction for NO_x is 1143 t, which is a 77% reduction of emissions in the inner city zone and a total reduction of 17% of all road traffic emissions, which leads to a remaining traffic contribution of 5739 t NO_x (32%) in the "inner city zone" scenario. The reduction for $PM_{2.5}$ is 51 t, which is a 14% reduction of emissions in the inner city zone and a total reduction of 3% of all road traffic emissions, which leads to a remaining traffic contribution of 1533 t $PM_{2.5}$ (63%) in the inner city scenario. The smaller reductions of $PM_{2.5}$ arise from contributions of brake and tire wear as well as resuspension from streets, which are not projected to decrease due to a change in fleet composition, while exhaust gas related PM emissions are substantially decreasing. Nevertheless, the uncertainties concerning non-exhaust emissions are still rather high in the projected emission reduction (Matthias et al., 2020) and further research is necessary for all the contributions, i.e. road dust resuspension, tire, brake, clutch and road wear. While for electrical cars it is still unknown to what extent recuperative braking reduces wear, their increased weight due to heavy batteries is considered to lead to significant contributions to PM emissions (Timmers and Achten, 2018). As exhaust emissions control become stricter, relative contributions of non-exhaust sources to traffic-related emissions will become more significant and may account for up to 90% of total PM emissions from traffic within a decade (e.g. Grigoratos and Martini, 2014).

The "land-powered ships" and "inner city zone" scenarios are simulated separately and in combination ("combined" scenario) to derive the changes in pollutant concentrations and population exposure compared to the "reference" situation in the year 2012 (section 3.4).

2.5. Exposure calculations

Population exposure estimates are used in epidemiological studies to evaluate health risks associated with the impacts of air pollution on human health. The principle idea of exposure is to account for the pollutant concentration values in the environments where people stay, and the amount of time they spend within them (WHO, 2006). There

exist several modelling approaches to implement this principle idea (Özkaynak et al., 2013). In this study, we used a simple static approach to account for population activity in European urban areas for exposure calculations. This approach takes into account the population counts at residential addresses of the urban population without any temporal or spatial variation.

Following this approach, we used gridded population counts of the population of Hamburg as derived from census 2011 with a grid resolution of 100 m (http://www.statistik-nord.de/fileadmin/maps/zensus2011_hh/). We then calculated the annual mean population exposure using the following

$$E_i = P_i \times \overline{C}_i \quad (1)$$

where E_i is the annual mean population exposure in grid cell i, P_i is the respective population number in grid cell i and $\overline{C}_i$ is the annual mean concentration of the pollutant in grid cell i. To be consistent with the gridded population dataset resolution, we disaggregated the simulated annual concentration to a 100 m resolution by resolving the 1 km × 1 km grid cells with the same values to 100 m × 100 m grid cells, before calculating the annual mean exposure. The annual mean population exposure in each grid cell was then displayed in maps. This metric can be used to identify hotspots of exposure. Based on the annual mean population exposure the population-weighted mean exposure (PWE) to pollutants is calculated as

$$\overline{E} = \frac{\sum_{i=1}^{n} E_i}{P} \quad (2)$$

where $\overline{E}$ is the population-weighted mean exposure for the population, n is the number of populated grid cells by a population, E_i is the mean exposure in grid cell i for the population and P is the respective total population. This exposure metric allows for the evaluation of exposure to annual concentrations of air pollutants at a city-scale population level. For both, the annual mean population exposure as well as the population-weighted mean exposure, the relative contributions from annual mean concentrations by traffic and shipping were identified.

3. Simulated NO_2 and $PM_{2.5}$ concentrations and estimated exposure

3.1. Evaluation of modelled concentrations

Hourly reference run results for NO_2 and $PM_{2.5}$ including all emission sources in 2012 have been compared to hourly air quality data from the HaLM at 13 NO_2 and 4 $PM_{2.5}$ measurement sites (Table 3, Figs. B1 and B2). An introduction into the statistical parameters used for evaluation can be found in annex A. Comparisons of time series can be found in annex B, while hourly, weekday and monthly time variations for modelled versus measured NO_2 and $PM_{2.5}$ can be found in Supplement I.

The NO_2 evaluation (Fig. 4a) reveals two characteristic groups of stations: (1) correlations below 0.4 and variations in normalized standard deviation below one and (2) correlations above 0.4 and variations in standard deviation above one. The first group consists exclusively of near road stations. The performance for $PM_{2.5}$ (Fig. 4b) can only be evaluated with four stations. Correlations are above 0.4 for all stations. We grouped the available stations (Table 3) in categories of background, urban and near road stations and calculated mean statistical indicators (Table 4) with the JRC Fairmode Delta Tool v5.6 (Monteiro et al., 2018). The statistical evaluation of annual $PM_{2.5}$ concentrations exhibits good model performance with Pearson correlation coefficients of $r \geq 0.5$. The model tends to underestimate $PM_{2.5}$ concentrations at urban stations (13ST, 20VE, 61WB) with an NMB of −11%. At the only near road station (64 KS), the model highly underestimates the measured concentrations with an NMB of −38%. When it comes to NO_2, the model performs well at urban and background stations with correlation coefficients of $r \geq 0.5$. The NO_2 concentrations are underestimated at one background station with a NMB of −18%, are slightly underestimated at urban stations with a mean NMB of −7% and are highly underestimated at near road stations with a mean NMB of −54%. Thus, the TAPM simulations underestimate concentrations near roads, which is mainly because the model does not resolve urban features such as street canyons. Nevertheless, all groups of stations for both pollutants show FAC2 values far above 0.3, which satisfies the FAIRMODE acceptance criteria of FAC2 ≥ 0.3 for urban dispersion model evaluation (Hanna and Chang, 2012).

Besides comparisons against measurements, we compared similar TAPM simulations for Hamburg in the year 2012 to evaluate the performance of concentrations simulated with TAPM. Karl et al. (2019) compared modelled results from TAPM simulations with a 1 km horizontal grid resolution for Hamburg 2012 to results modelled with the urban-scale CTM EPISODE-CityChem (Karl and Ramacher, 2018), based on a similar set of emissions, meteorology and boundary conditions. Besides a better performance of EPISODE-CityChem at traffic stations Karl et al. (2019), TAPM showed low bias and relatively good correlation for NO_2 at the industrial sites and stations influenced by emissions from industry and shipping, similar to EPISODE-CityChem. For PM at urban background stations, EPISODE–CityChem performed slightly better than TAPM in terms of correlation and IOA, due 3-D boundary conditions instead of 2-D boundary conditions, while urban stations performed similar to EPISODE-CityChem. Karl et al. (2019) evaluated the models in terms of fitness for purpose (Thunis et al., 2012; Monteiro et al., 2018) for NO_2 (hourly) and PM_{10} (daily mean). For EPISODE–CityChem, the data indicate fulfilment for all pollutants at all stations, while for TAPM the same holds true at urban and background stations. Nevertheless, at traffic stations TAPM shows an error dominated by bias.

3.2. Contributions of traffic and shipping

In a first step, we compared the modelled annual mean

Table 3
Hamburger Luftmessnetz (HaLM) measurement stations with type of stations and measured pollutant. See Fig. 2a for a map of station locations.

Station Code	Station Name	Station Type	Altitude	Lon	Lat	Pollutants Measured
13ST	Sternschanze	Urban	3.5	9.96834	53.56449	NO_2, O_3, PM_{10}, $PM_{2.5}$, SO_2
17SM	Stresemannstrasse	Traffic	1.5	9.957387	53.56086	NO_2, O_3, PM_{10}
20VE	Veddel	Urban	3.5	10.02197	53.52291	NO_2, PM_{10}, $PM_{2.5}$, SO_2
21BI	Billbrook	Urban	3.5	10.08214	53.52943	NO_2, PM_{10}, SO_2
27 TA	Tatenberg	Urban	3.5	10.08365	53.48814	NO_2, O_3
51BF	Bramfeld	Urban	3.5	10.1105	53.63089	NO_2, O_3
52NG	Neugraben	Background	3.5	9.857199	53.48098	NO_2, O_3
61WB	Wilhelmsburg	Urban	3.5	9.990543	53.50792	NO_2, PM_{10}, $PM_{2.5}$, SO_2
64 KS	Kielerstrasse	Traffic	1.5	9.944616	53.56437	NO_2, $PM_{2.5}$
68HB	Habichtstrasse	Traffic	1.5	10.05372	53.59235	NO_2, PM_{10}
70 MB	MaxBrauerAllee	Traffic	1.5	9.943065	53.55573	NO_2, PM_{10}
74BT	Billstedt	Urban	3.5	10.10286	53.53851	NO_2, PM_{10}
80 KT	AltonaElbhang	Urban	3.5	9.944915	53.54524	NO_2, O_3, PM_{10}, SO_2

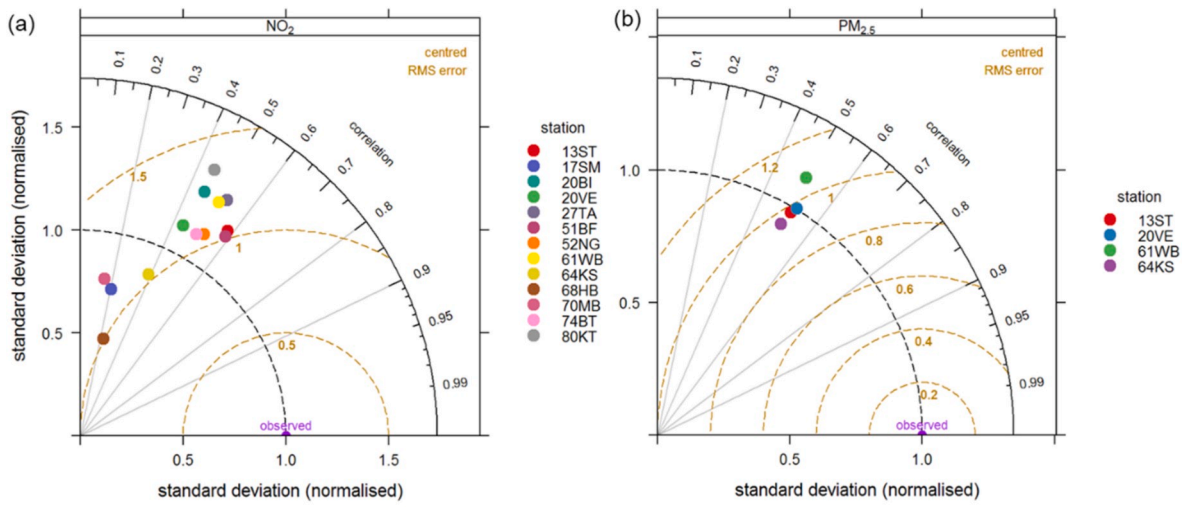

Fig. 4. Taylor Plots of hourly measured vs. modelled NO_2 and $PM_{2.5}$ concentration in Hamburg at all available HLM stations.

Table 4
Annual model performance statistics of TAPM simulations for NO_2 and $PM_{2.5}$ in Hamburg based on hourly concentrations in 2012, and grouped by station types (derived with JRC Fairmode Delta Tool v5.6). Indicators are introduced in annex B.

Station type	Pollutant	n [#]	$Mean_{obs}$ [µg m-3]	$Mean_{mod}$ [µg m-3]	sd_{obs} [µg m-3]	sd_{mod} [µg m-3]	FAC2 [-]	NMB [-]	RMSE [µg m-3]	r [-]	IOA [-]
Background	NO_2	8345	14.9	12.3	12	14	0.65	−0.18	13	0.52	0.56
Urban	NO_2	68441	27.8	25.8	17	20	0.71	−0.07	18.3	0.53	0.52
Street	NO_2	34434	58.9	26.8	30	20	0.41	−0.54	45	0.22	0.26
Urban	$PM_{2.5}$	16920	12.6	11.3	8.5	9.4	0.75	−0.11	8.8	0.51	0.52
Street	$PM_{2.5}$	8664	18.4	11.5	9.2	8.2	0.56	−0.38	11	0.51	0.33

concentrations with annual mean measurements at all available stations and additionally highlighted the modelled sectoral contributions (Fig. 5). In Fig. 5a, we show all stations for NO_2. While the total modelled values match the measured values quite well (except for high underestimations at traffic sites), the spatial differences in the contribution of shipping and traffic related concentrations are quite visible in the analysis. At station 80 KT, which is close to the port area, the modelled impact of shipping on NO_2 concentrations is responsible for 50% of the total concentration, while at other stations in the city the impact ranges from 3% to 30%. The impact of road transport is between 3 and 25% at all stations for NO_2, although higher contributions at traffic stations could be expected. For $PM_{2.5}$, shipping and traffic have less variability in their spatial distribution with contributions of 20% for traffic and 4% for shipping on average. The annual mean $PM_{2.5}$ concentration at the traffic station 64 KS is highly underestimated. The modelled regional contribution to $PM_{2.5}$ concentrations at all stations varies from 60 to 75%.

In a second step, we created maps of annual mean NO_2 and $PM_{2.5}$ concentration of the urban domain in Hamburg for the year 2012 as well as maps showing the relative impact of traffic and shipping (Fig. 6). While local NO_2 maxima (up to 75 µg m^{-3}) of annual mean concentrations are widespread in the port area and industrial areas nearby, the

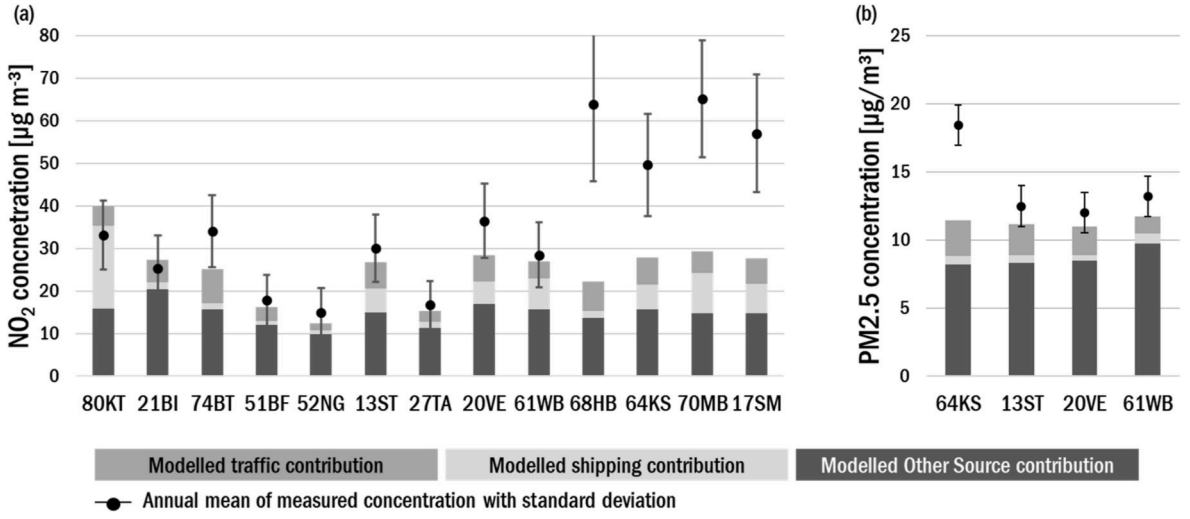

Fig. 5. Annual mean modelled vs. measured NO_2 and $PM_{2.5}$ concentration including sectoral contributions of road traffic and shipping at selected measurement stations of HaLM.

$PM_{2.5}$ concentration maxima (up to 33 μg m^{-3}) in the Hamburg area are focused on the port and industrial area of Hamburg. These hot spot areas are mainly influenced by emissions released from industrial sources. In addition, with up to 60% for NO_2 and 30% for $PM_{2.5}$ shipping contributes significantly to the high concentrations in this area. Traffic related NO_2 and $PM_{2.5}$ concentrations are very low in these hotspots. They are concentrated around highways and in the city centre, with high contributions in the city centre (30%) and decreasing impacts towards the outskirts (10%). In general, the local contributions of transport emissions to NO_2 concentrations are higher than for $PM_{2.5}$ due to the importance of long-range transport for $PM_{2.5}$. Moreover, when it comes to shipping, the $PM_{2.5}$ concentrations are more focused and less wide spread with distance to the port area. For NO_2 from shipping, residential areas within a distance of 5 km from the port area still experience contributions of shipping emissions to air pollution of 20–30%. Moreover, although high traffic contributions to NO_2 are found near highways, the urban centre and residential areas are also widely influenced by traffic with contribution of 30–40%.

In a third step, we analysed the exceedances of EU and WHO limits for modelled NO_2 and $PM_{2.5}$ and compared these to measured exceedances at measurement stations related to the specific grid cells. The results are summarized in Table 5. In Fig. 6a and d the exceedances of annual limits for NO_2 and $PM_{2.5}$ as defined by the EU directive, becomes visible with the highest colour coding (yellow). For NO_2 and $PM_{2.5}$, exceedances mainly occur in the vicinity of the port and industrial areas located in the south of the port area. When it comes to NO_2, there have been four exceedances of annual limits (40 μg/m^3) measured. The TAPM simulations show one exceedance in grid cells which relate to measurement stations. Analysing the hourly limit of 200 μg/m^3 there are five exceedances measured and nine exceedances modelled at locations close to the measurement stations. However, the NO_2 limit simulated with TAPM gives a number of exceedances for hourly NO_2 limits, which are very close to the number of exceedances at the monitoring stations. In the model domain, we simulated in total 775 hourly NO_2 limit exceedances. Most of these exceedances are located at the north side of the river Elbe, close to the port area.

For $PM_{2.5}$ there haven't been exceedances of the EU's annual limit of 25 μg/m^3 measured and modelled but looking at the WHO's limit of 10 μg/m^3 there are four exceedances measured and modelled at respective measurement stations. Besides the analysis of simulated concentrations in grid cells representing measurement stations, we also analysed simulated exceedances in all grid cells of the research domain. In the total research domain, we modelled.

Table 5
Measured and modelled exceedances and number of people exposed to hourly and annual NO_2 as well as annual $PM_{2.5}$ concentrations above limits by EU and WHO. For modelled exceedances of hourly NO_2 values, the sum of all grid cells, which exceed the limit, is shown. Therefore, it could be the same grid cell repeatedly but for different hours.

Pollutant	NO_2		$PM_{2.5}$	
Type	hourly	annual	annual	annual
Limit	200 μg/m^3	40 μg/m^3	25 μg/m^3	10 μg/m^3
Regulation	EU/WHO	EU/WHO	EU	WHO
Total measured exceedances at measurement stations	5	4	0	4
Total modelled exceedances in grid cells representing stations	9	1	0	4
Total modelled exceedances in all grid cells of the domain	775	18	1	601
Population exposed to at least one exceedance	259,682	13,947	0	709,390
Share of population exposed to exceedances	14.28%	0.77%	–	39.01%

- 775 exceedances of hourly NO_2 limits by EU and WHO,
- 18 exceedances of annual NO_2 limits by EU and WHO,
- 1 exceedance of annual $PM_{2.5}$ limits by EU and
- 601 exceedances of annual $PM_{2.5}$ limits by WHO.

Taking into account the number of people who are living in areas contained in the model domain, there are about 14% of the population of Hamburg exposed to hourly NO_2 concentration above the limit, <1% to annual NO_2 concentrations above the limit, and 39% are exposed to $PM_{2.5}$ concentrations above the WHO limit.

3.3. Annual mean population exposure to traffic and shipping

To gather insights of the spatial variability of sectoral contributions to average concentrations and to concentration maxima, it is necessary to consider the exposure of population to air pollution in total and by

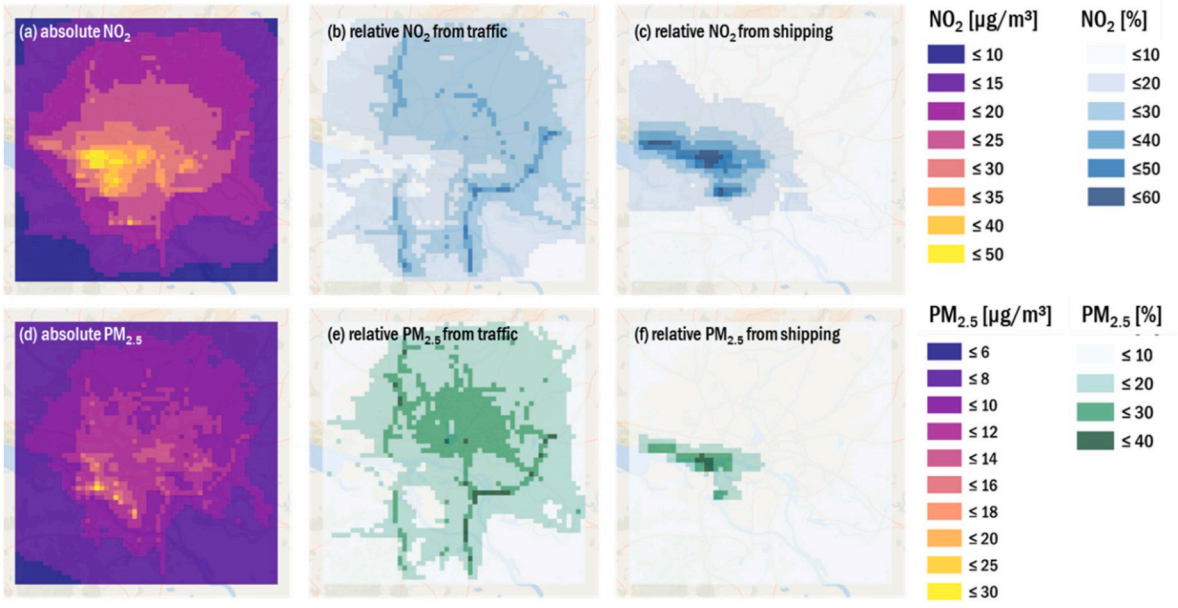

Fig. 6. Annual mean modelled NO_2 and $PM_{2.5}$ concentration and relative contributions from road traffic and shipping.

emission source. Using the simulated NO_2 and $PM_{2.5}$ concentrations, the total population exposure has been calculated by multiplying disaggregated concentration grids with total gridded population at 100 × 100 m^2 resolution. Fig. 7a and d shows the annual mean exposure to NO_2 and $PM_{2.5}$ from all sources. In comparison to the concentration maps (Fig. 6), it can be seen, that there are no exposure hotspots in areas with concentration maxima in the port and industrial area south of the river Elbe. Nevertheless, the residential areas close to the port area north of the river Elbe show highest exposure levels to NO_2 and $PM_{2.5}$. For $PM_{2.5}$, the spatial distribution of concentration hotspots coincides with residential areas, which are densely populated in the suburbs of Hamburg around the city centre. Moreover, the densely populated island and district of Wilhelmsburg in south-central Hamburg, close to the port area, shows high levels of exposure to $PM_{2.5}$.

The traffic sector contributes 15% in the outskirts and up to 30% in the centre to the $PM_{2.5}$ exposure (Fig. 7e) all over the city, while shipping has a big impact at the north west side of the river Elbe (Fig. 7f). In general, the patterns of relative exposure from traffic and shipping follow the patterns of relative concentration impacts from traffic and shipping.

The calculation of the population-weighted mean exposure to NO_2 and $PM_{2.5}$ (Table 6) reveals mean exposures of 20.51 μg/m^3 for NO_2 and 9.42 μg/m^3 for $PM_{2.5}$ (Table 6). In terms of PWE to NO_2, traffic contributes 22.7% and is 1.6 times higher than shipping contributions, which are 13.9%. In total, traffic and shipping contribute 36.6% to the PWE in Hamburg 2012). When it comes to $PM_{2.5}$, traffic contributes 18.1% and is 5.3 times higher than contributions from shipping, which account for 3.4%. In total, traffic and shipping contribute 21.5% to the PWE in Hamburg 2012).

3.4. Concentration and exposure results for emission reduction scenarios

The results of simulated emission reduction scenarios are analysed in terms of their contribution to the mean concentrations (Table 7a), their contribution to the simulated exceedances of pollutant concentration limits (Table 7b) as well as their impact on total population exposure (Figs. 8 and D1) and PWE.

The annually averaged domain concentrations of NO_2 and $PM_{2.5}$ are slightly decreased in all scenarios. The highest reduction for NO_2 is achieved in the "land-powered ships" scenario (−8.2%), while the "inner city zone" scenario leads to a −2.9% decrease (Table 7a). $PM_{2.5}$ is reduced by −3.1% in the "land-powered ships" scenario and by −1.7% in the "inner city zone" scenario. Nevertheless, the annually averaged grid means are not taking into account the spatial distribution of changes in concentrations.

Table 6
Population-weighted mean exposure to NO_2 and $PM_{2.5}$ for baseline, traffic and shipping.

Hamburg 2012	Baseline	Traffic		Shipping		Traffic/ Shipping
	μg m^{-3}	μg m^{-3}	% of baseline	μg m^{-3}	% of baseline	[-]
NO_2	20.51	4.65	22.7%	2.86	13.9%	1.6
$PM_{2.5}$	9.42	1.70	18.1%	0.32	3.4%	5.3

The results for the scenario impacts on modelled exceedances (Table 7b), shows substantial reductions for all scenarios and both pollutants. For both pollutants the highest reductions of modelled limit exceedances are in the "land-powered ships" scenario, with reduction of −75% for hourly NO_2, -100% for annual NO_2 and -27% for $PM_{2.5}$ (WHO limit).

When combined with the "inner city zone" scenario the number of modelled exceedances is reduced by −81% for hourly NO_2 and -38% for annual $PM_{2.5}$ (WHO limit). Therefore, the population that is exposed to exceedances of pollutant concentration limits could potentially be reduced by −91% in terms of hourly NO_2, -100% in terms of annual NO_2 and -50% in terms of annual $PM_{2.5}$ (WHO limit). When it comes to the annual EU $PM_{2.5}$ limit, there is no change modelled for the single exceedance, which occurs on the port area, where no population is present.

Fig. 8 shows the change in absolute values of total exposure in all scenarios, while Figure D1 (annex D) shows the relative changes in total exposure for all scenarios. For both, NO_2 and $PM_{2.5}$ the highest absolute and relative reductions are modelled in the densely populated areas north of the port area, with relative reductions in total exposure of up to −35% for NO_2 and -30% for $PM_{2.5}$. This is also the area, where most exceedances have been modelled in the reference scenario and thus are reduced in the modelled scenarios (Table 7b). The area of impact for the land-powered ships scenario is limited to the surroundings of the port area, especially for $PM_{2.5}$. Nevertheless, there have been modelled small increases (maximum +5%) in exposure to NO_2, especially close to the model domain's boundaries. This is probably due to a shift in the local chemistry regimes, when NO_x emissions from shipping are substantially decreased in the port area and interactions with e.g. background O_3 are changing. The impact on total exposure is rather small, due to sparsely populated areas in the urban area's surroundings close to the domain

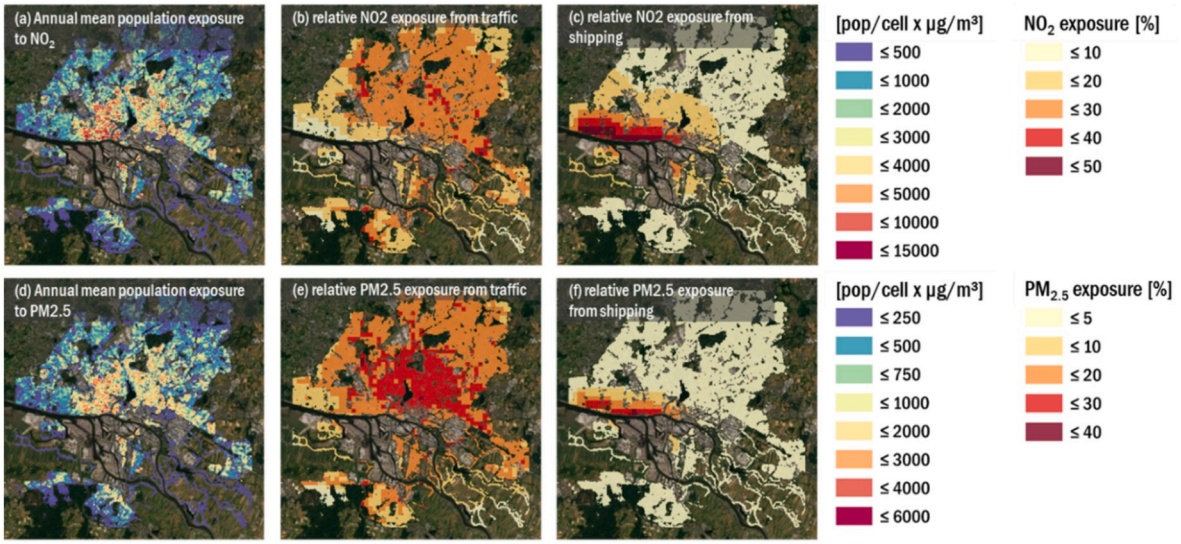

Fig. 7. Modelled annual mean population exposure to NO_2, $PM_{2.5}$, and relative contributions from road traffic and shipping.

Table 7a
Annually averaged domain mean concentrations of NO_2 and $PM_{2.5}$ for the reference and all emission reductions scenarios.

Hamburg 2012	Reference	"land-powered ships"		"inner city zone"		"combined"	
	μg m^{-3}	μg m^{-3}	% reduction	μg m^{-3}	% reduction	μg m^{-3}	% reduction
NO_2	16.82	15.42	−8.2%	16.02	−4.8%	15.23	−9.5%
$PM_{2.5}$	8.43	8.17	−3.1%	8.29	- 1.7%	8.12	−3.7%

Table 7b
Changes in Population-weighted mean exposure to NO_2 and $PM_{2.5}$ for all scenarios.

Modelled exceedances	NO_2 hourly	NO_2 annual	$PM_{2.5}$ annual (EU)	$PM_{2.5}$ annual (WHO)
2012 Reference	775	18	1	601
"land-powered ships" scenario	194 (−75%)	0 (−100%)	1	440 (−27%)
"inner city zone" scenario	636 (−18%)	14 (−22%)	1	510 (−15%)
"combined" scenario	147 (−81%)	0 (−100%)	1	373 (−38%)

Table 8
Comparison of different datasets for gridded population density.

Population dataset	reference PWE [μg/m^3]	
	NO_2	$PM_{2.5}$
Census data 2011	20.51	9.42
Population density from Urban Atlas 2012 (Batista e Silva and Poelman, 2016)	19.80 (−3.5%)	9.19 (−2.4%)
Global Human Settlement Map (Florczyk et al., 2019)	19.98 (−2.6%)	9.28 (−1.5%)

border.

The reductions modelled in the "inner city zone" scenario have mostly an impact on the inner city zone itself, but merely in the surroundings for $PM_{2.5}$, with reductions of up to −7% in maximum, which is due to the small reductions in $PM_{2.5}$ emissions. For NO_2, the reductions can reach up −18% in the inner city zone and have an impact up to −4% in the rest of the domain. When both scenarios are combined highest reduction potentials become visible with up to −10% for $PM_{2.5}$ in the inner city zone and up to −30% in the vicinity of the harbour. For NO_2 the results of the combined scenario show a reduction of up to −40% in the north of the port area and up to −25% in the inner city zone. The PWE to NO_2 in the scenario "combined" is reduced by −7% to 18.98 μg/m^3, while the PWE to $PM_{2.5}$ is reduced by −5% to −9 μg/m^3."

In total, all emission reduction scenarios reveal chances to decrease the population exposure in the metropolitan area of Hamburg with substantial reductions of limit value exceedances of hourly NO_2, annual NO_2 and annual $PM_{2.5}$.

4. Discussion of uncertainties

We calculated the population exposure to NO_2 and $PM_{2.5}$ concentrations in Hamburg for year 2012, with an urban-scale CTM system and a static exposure calculation approach. The applied models and methods used are subject to a number of uncertainties:

In terms of uncertainties within the applied CTM system, which is used to model concentrations, the range of uncertainty can be identified by comparisons with measurements. The evaluation of model results based on measurements (section 3.1) revealed in general a good model performance according to accepted statistical parameters, i.e. a small annual BIAS at urban and background stations. Nevertheless, modelled values highly underestimate the situation at traffic stations. The high underestimation of traffic concentrations is mainly due to low grid-resolution of 500 × 500 m^2 in the TAPM simulations, which is not capable of reproducing streets and street canyons. Moreover, TAPM does

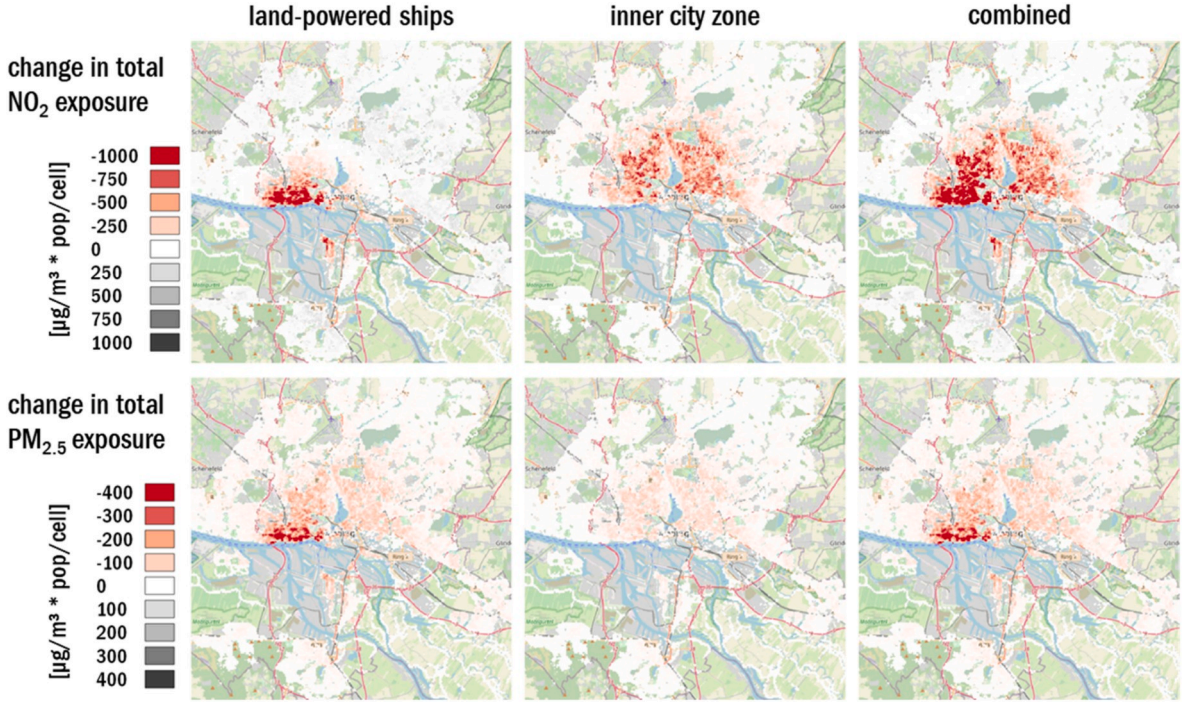

Fig. 8. Modelled changes in total NO_2 and $PM_{2.5}$ exposure in the scenarios land-powered ships, inner city zone and combined.

not account for street canyon effects, i.e. higher or lower ventilation, leading to trapped pollutants in narrow canyons. Although TAPM shows good agreement with modelled and measured exceedances in this study, it should be taken into account that most exceedances of hourly NO_2 limits are expected at traffic stations, which are those stations, where TAPM shows high underestimations. Thus, the reliability of modelled short-term exposure to hourly exceedances of NO_2 should not be overrated. The modelled results might be right for the wrong reason. Future studies to investigate urban air pollution should take into account the effect of street canyons, e.g. by applying a simplified street canyon model within a CTM setup, as it is used e.g. in the EPISODE-CityChem model by Karl et al. (2019).

Another argument for the application of further developed urban-scale CTM systems, is the simple GRS chemistry mechanism in TAPM, which has been challenged in the past (Tonnesen and Jeffries, 1994). The GRS chemistry scheme is an empirical parameterization, which has been developed with the primary aim to reproduce O_3 concentrations in Australian smog chamber experiments. At VOC-to-NOx ratios greater than 8:1, the GRS is capable of reproducing NO_x and O_3 profiles also under atmospheric conditions. However, at low VOC-to-NO_x ratios that are typical for inner-city urban air, GRS tends to predict higher O_3 maxima than more comprehensive chemistry mechanisms. Specifically, GRS does not include features needed to represent the effect of NO_x inhibition of radical formation that prevail at high NO_x levels. In an recently published study, TAPM results for modelled O_3 concentrations in Hamburg have been compared to the more sophisticated urban-scale model EPISODE-CityChem (Karl et al., 2019) that entails a rather detailed atmospheric chemistry mechanism, originally based on the EMEP chemistry scheme (Walker et al., 2003; Simpson et al., 2012). The performance of TAPM to reproduce the temporal variability of the daily maximum 8h running mean O3 concentrations at several urban monitoring sites was only slightly worse than that of EPISODE-CityChem. Considering the limitations of GRS chemistry in dealing with the high variability of chemistry regimes on urban scales, it becomes evident, that urban-scale CTM systems with more recent and reliable chemistry mechanism should be considered to simulate urban air quality, to eliminate this source of uncertainty.

Additionally, Matthias et al. (2018) and Bieser et al. (2020) showed that the biggest uncertainty in CTM simulations is mostly due to shortcomings in emission inventory data. Especially in urban areas, concentrations of NO_x and $PM_{2.5}$ heavily depend on local emissions because of the spatial proximity of emission sources and the relative insignificance of sinks due to the short retention time of urban air masses. Modelling the magnitude, temporal distribution and spatial distribution of emissions is often connected with high uncertainties and thus has a high influence on the CTM results. For example, uncertainties in VOC emissions will result in uncertainties of NO_2 concentrations. The formation of ozone from NO_x and volatile organic compounds from traffic and other urban sources represents one of the major uncertainties in the field of atmospheric chemistry, especially in urban areas Sillman (1999). In TAPM, the concept of using the variable Rsmog rather than the concentration of Volatile Organic Compounds in the reaction equations is applied. The concentration of Rsmog is defined as a reactivity coefficient multiplied by VOC concentrations. For example, Johnson (1984) used [Rsmog] = 0.0067 [VOC] for typical 1980s Australian urban air dominated by motor vehicles. This empirically determined reactivity coefficient is not available for Hamburg and thus we used the same RSmog value of 0.0067. However, it might not be suitable for conditions in Hamburg and therefore leading to both, uncertainties in the VOC emissions as well as the representation of VOC in the reaction equations for NO_x formation.

Additionally, traffic NO_2 and $PM_{2.5}$ emissions are likely to be underpredicted in our emissions inventory compiled for Hamburg in the year 2012. Although these are based on traffic counts and were modified as described in section 2.3, they do not account for effects of traffic congestion, slowing down of traffic in certain locations and streets and the effects of idling, cold starts, and the deceleration and acceleration of vehicles. Traffic congestion can increase emissions in streets during rush hours (Smit et al., 2008; Gately et al., 2017; Requia et al., 2018). Moreover, Kuik et al. (2018) report that many modelling studies show underestimations of modelled NO_x and NO_2 compared with observations, which can partly be attributed to an underestimation of NO_x emissions, particularly in urban areas. This is consistent with recent measurement studies quantifying underestimations of urban NO_x emissions by current emission inventories, identifying the largest discrepancies when the contribution of traffic NO_x emissions is high. Kuik et al. (2018) suggest that an underestimation in traffic emissions is likely one of the main causes of the bias in modelled NO_2 concentrations in the urban background. In general, Kuik et al. (2018) suggest that more research is needed in order to more accurately understand the spatial and temporal variability in real-world NO_x emissions from traffic, and apply this understanding to the inventories used in high-resolution CTM. When it comes to $PM_{2.5}$ concentrations in urban areas, these are strongly impacted by the long-range transport of material emitted outside the urban area and transported over considerable distances and therefore, lower contributions of local sources can be expected. Nevertheless, the high underestimations of $PM_{2.5}$ near roads in this study might also be due to missing $PM_{2.5}$ emission in the emission inventory, missing tyre, break, and road wear emissions or missing representation in resuspension of particles. Thus, in future studies we plan to improve the emissions inventory for road traffic, e.g. by integrating the effects of traffic-congestion based on traffic counts and analysis of measurements at road traffic sites. Moreover, we aim to adapt the temporal profiles of daily road traffic based on measurements at road traffic sites as proposed by Kuik et al. (2018). Finally, we plan to take into account specific emission factors for non-exhaust emissions as e.g. presented by van der Denier Gon et al. (2018). In total, the exposure to traffic is very likely to be under-predicted at near road locations in this study due to an underestimation of emissions sources for transport related NO_x and $PM_{2.5}$ emissions.

When it comes to the applied bottom-up approach to account for shipping emissions, the calculated emissions depend mainly on emission factors for different modes of activity (e.g. sailing, manoeuvring, and berthing). In this study the calculation of emissions that arise from the use of auxiliary engines, while ships are at berth is likely to be a source of high uncertainty in the shipping emissions, because little is known about the use of auxiliary engines. Hulskotte and Denier Van Der Gon (2010) gained their fuel consumption and emission factors by evaluating surveys carried out with ship engineers and captains. These were applied in the bottom-up approach of this study. Given the limited number of ships they could explore, it is difficult to estimate the accuracy of the resulting emissions used in this study. Nevertheless, we judge the calculated shipping emissions in total to be robust because the calculated total emissions from shipping are below total emissions as reported for 2012 (section 2.3). The comparison of modelled and measured NO_2 concentrations revealed a slight over prediction at the 80 KT site (Fig. 4), which is closest to the port area and shows a modelled contribution of shipping of up to 50%. This might indicate an overestimation of simulated NO_2 concentrations by shipping in the area close to the port, which is also the area that revealed high reduction potentials for exposure and limit exceedances, when decreasing emissions from shipping at berth. A possible explanation could be the vertical distribution of shipping emissions. In this study, shipping emissions are released in the lowest vertical layer of the model. In future studies a better representation of ship's stack heights should be considered, e.g. by using averaged stack heights derived from available ship characteristics. In terms of $PM_{2.5}$, there might be additional uncertainties due to the reduced representation of the formation of secondary particulate matter (SPM) in TAPM by taking into account stable non-gaseous organic carbon (SNGOC), stable non-gaseous nitrogen products (SNGN) and stable nongaseous sulphur products (SNGS). Primary air pollutants from shipping contribute to the formation of secondary air pollutants, mainly ozone and secondary

particulate matter. In the chemistry mode of TAPM, the simplified chemical reactions for SPM are included and the secondary particulate matter consists of organic carbon, nitrogen products and sulphur products. Tang et al. (2020) showed in a TAPM modelling study for the Gothenburg urban area low modelled SPM concentrations from shipping but since SPM is usually formed further from the sources, the higher SPM can disperse 5–10 km downwind of the ship emissions.

Meteorological fields – mainly wind flow fields and air temperature – and regional boundary conditions are also crucial inputs for correct CTM simulations. Nevertheless, Karl et al. (2019) proved good agreement with measurements for the regional boundary conditions as calculated with CMAQ, and the performance of the meteorological module of TAPM shows very good agreements with measurements. Therefore having correct emissions is the highest priority in terms of improving the concentrations of NO_2 and $PM_{2.5}$ with TAPM, which then will linearly improve the results of exposure calculations.

When it comes to the applied static exposure approach, the underlying assumption is that people are at residential addresses throughout the time. Thus, static exposure does not account for the spatial and temporal variability of population activities and will lead to uncertainties in calculated exposure and introduce potential bias in the quantification of human health effects, as the individual and population-level mobility is not accounted for. Several exposure modelling studies have overcome this traditional approach and are using population activity data, derived from surveys, individual GIS data or generic data, and models to account for the diurnal variation in population numbers in different locations (e.g. (Bell, 2006; Beckx et al., 2009; Beevers et al., 2013; Soares et al., 2014; Reis et al., 2018; Ramacher et al., 2019; Xu et al., 2019). Thus, to model population numbers suitable for exposure calculations, it is generally necessary to know the population distribution and characterisation and therefore the number of people and diurnal activity patterns of different characteristic population groups. This information was missing for Hamburg and thus we decided to apply a static exposure approach. In future studies we plan to account for population dynamics by applying population activity profiles, which are additionally diversified by demographic groups in different microenvironments, such as residential environments, work environments or traffic environments. This additionally allows for the utilisation of microenvironment specific consideration of outdoor concentrations infiltrating into indoor environments and thus a better representation of pollutant concentrations people are exposed to.

Due to the application of a static exposure, the gridded population becomes a crucial dataset for the estimation of exposure. In this study, we applied gridded census data with a 100 m horizontal resolution (http://www.statistik-nord.de/fileadmin/maps/zensus2011_hh/). This dataset is also used by the municipality of Hamburg and to our knowledge this is the best available dataset for population distribution in the Hamburg metropolitan area. Nevertheless, we compared this dataset with two other frequently used datasets of gridded population for the same reference year, to derive the impact of population datasets on urban-scale population exposure estimates (Table 8). Assuming, that the high-resolution dataset from the census data is the most representative dataset available, the comparison shows slightly lower estimates of PWE compared to a dataset, which is based on European data for disaggregation of census data from the Copernicus Urban Atlas 2012 (Batista e Silva and Poelman, 2016) and for a dataset, derived from the Global Human Settlement Map (Florczyk et al., 2019). The relative changes are also valid for the estimation of total exposure sums.

In this study, we applied the most representative available emission and population data, which was for year 2012. Due to mostly linear and slow decreases in emissions, we evaluate the simulated sectoral contributions of traffic and shipping, as well as the scenario results as qualitative results to be transferable to recent years. Especially the potential emission reduction is a valuable outcome for recent years.

Despite these limitations and in the light of possibilities for improvement in the urban-scale CTM system and exposure calculations, we are convinced of the applicability of the presented urban-scale CTM system for the evaluation of urban air quality to support local authorities and health-effect studies. Nevertheless, future health-effect studies could highly benefit from detailed uncertainty analyses of simulated pollutant concentrations and population exposure they are based upon.

5. Conclusions

We investigated the contribution of road traffic and shipping related emissions of NO_2 and $PM_{2.5}$ to air quality and annual mean population exposure in Hamburg for the year 2012. For this purpose, we compiled a detailed emission inventory for all emission sources following SNAP categories. The emission inventory was applied in an urban-scale Chemistry Transport Model system to simulate hourly NO_2 and $PM_{2.5}$ concentration with a horizontal grid resolution of 500 m. To simulate urban-scale pollutant concentrations we used the coupled prognostic meteorological and chemistry transport model TAPM. The comparison of modelled with measured hourly values shows good correlations and low biases at urban and background stations but high underestimations of NO_2 and $PM_{2.5}$ concentrations at measurement stations near roads.

The simulation results for annual mean population exposure from road traffic and shipping revealed that the traffic sector contributes 15% in the urban outskirts and up to 30% in the urban centre to the $PM_{2.5}$ exposure, while shipping has a big impact north of the river Elbe. In terms of modelled exceedances of limits, NO_2 and $PM_{2.5}$ exceedances mainly occur near the port and industrial areas located in the south of the port area. Our simulation results for 2012 resulted in 14% of the population of Hamburg exposed to hourly NO_2 concentration above the hourly limit of 200 $\mu g/m^3$, <1% to annual NO_2 concentrations above the limit of 40 $\mu g/m^3$, and 39% are exposed to $PM_{2.5}$ concentrations above the annual WHO limit of 10 $\mu g/m^3$. In terms of simulated exposure, residential areas close to the port area north of the river Elbe show the highest exposure levels to NO_2 and $PM_{2.5}$. In general, the patterns of relative exposure from traffic and shipping follow their patterns of relative concentration impacts from traffic and shipping. Nevertheless, the highest levels of NO_2 and $PM_{2.5}$ concentrations have been modelled in areas without population. The calculation of the population-weighted mean exposure to NO_2 and $PM_{2.5}$ reveals mean exposures of 20.51 $\mu g/m^3$ for NO_2 and 9.42 $\mu g/m^3$ for $PM_{2.5}$. In terms of PWE to NO_2, traffic contributes 22.7% and is 1.6 times higher than shipping contributions, which are 13.9%. In total, traffic and shipping contribute 36.6% to the PWE in Hamburg 2012). When it comes to $PM_{2.5}$, traffic contributes 18.1% and is 5.3 times higher than contributions from shipping, which are 3.4%. In total, traffic and shipping contribute 21.5% to the PWE in Hamburg 2012). Additionally, we created two local emission reduction scenarios and simulated these in the urban-scale CTM system. The results for a scenario that reduces all emissions from shipping at berth to zero, due to extensive use of on-shore electricity, revealed highest reduction potentials for NO_2 and $PM_{2.5}$ in terms of reductions to exceedances of pollutant concentration limits, total exposure and PWE.

The discussion of uncertainties revealed a high potential for improving the emissions inventories, chemical transport simulations and exposure calculations. There is more research needed in order to improve NO_x and $PM_{2.5}$ emission inventories from traffic and shipping, their accurate representation in CTM, as well as a more realistic consideration of population activity in exposure calculations. Therefore, in future studies we will take into account the effects of street canyons and a better representation of secondary particle formation as well as improved VOC chemistry in the reaction equations. Besides this, we plan to improve the emissions inventory for road traffic, e.g. by integrating the effects of traffic-congestion, adapting temporal profiles of daily road traffic based on measurements at road traffic and taking into account specific emission factors for non-exhaust emissions. For shipping emissions, we will apply more realistic vertical profiles to distribute emissions from shipping. When it comes to improvements in the exposure calculation, we plan to account for population dynamics by applying

averaged generic population activity profiles, which are additionally diversified by demographic groups in different microenvironments, and the utilisation of microenvironment specific consideration of outdoor concentrations infiltrating into indoor environments.

Due to the use of exposure calculations in health-effect studies, it is indispensable to reduce and quantify uncertainties for a better evaluation and interpretation of health-effects related to air pollution from different emission sources. The greatest benefit of the applied urban-scale CTM system and exposure calculation setup presented here is the possibility to use it for identifying most relevant emission sources and exposure hotspots. This information can be used for policy decisions and urban air quality management. Moreover, future studies aiming at the support of policy decisions could use the set up to create and evaluate sophisticated emission scenarios.

5.1. Data availability

The following data sets are available for download from the HZG ftp server upon request: (1) input data for the one-year AQ simulations of Hamburg (full set ca. 50 GB); (2) DELTA Tool data for comparison of model output and measurements; (3) model output data of the AQ simulations of Hamburg (full set ca. 50 GB); (4) model input and output data of the exposure calculations for all microenvironments of Hamburg (full set ca. 50 GB).

Author contribution

MOPR: Wrote the main text of the paper; developed the scientific questions; ran the model scenarios; analysed and evaluated the TAPM model results presented in this work; visualisation and plotting. VM: Supported scientific design of the case study. Text review. AA: Data and text contributions on shipping emissions. MQ: Supported scientific design of the case study. Text review. JB: Supported preparation and analysis of emission inventories. MK: Integration of TAPM emission input format in the UECT; text reviews; improvement of traffic emission inventories; provided technical and scientific guidance.

Declaration of competing interest

The authors declare that they have no known competing financial interests or personal relationships that could have appeared to influence the work reported in this paper.

CRediT authorship contribution statement

Martin Otto Paul Ramacher: Conceptualization, Data curation, Formal analysis, Investigation, Methodology, Software, Validation, Visualization, Writing - original draft. **Volker Matthias:** Formal analysis, Investigation, Supervision, Validation, Writing - review & editing. **Armin Aulinger:** Data curation, Formal analysis, Investigation, Methodology, Software, Writing - review & editing. **Markus Quante:** Formal analysis, Investigation, Supervision, Writing - review & editing. **Johannes Bieser:** Data curation, Formal analysis, Investigation, Software, Validation, Writing - review & editing. **Matthias Karl:** Formal analysis, Investigation, Methodology, Software, Supervision, Writing - review & editing.

Acknowledgements

We acknowledge CSIRO for distributing and providing support for TAPM. We acknowledge Stefan Nordmann and Stefan Feigenspan (UBA) for the preparation and distribution of emission datasets for Hamburg with the UBA GRETA tool. Moreover, we would like to thank Robert Schuldt (Behörde für Umwelt und Energie Hamburg) for the distribution of point source emission information. Copernicus Services is thanked for the public distribution of Urban Atlas, Corine Land Cover and population density products. We acknowledge ECMWF for ERA 5 synoptic reanalyses. Open Street Map is thanked for maps used in plots and David Carslaw is thanked for the Openair R-package, which was used to create Taylor Plots. The air quality model CMAQ is developed and maintained by the U.S. Environmental Protection Agency (US EPA). COSMO-CLM is the community model of the German climate research. The simulations with COSMO-CLM, CMAQ, EPISODE-CityChem and the exposure calculations were performed at the German Climate Computing Centre (DKRZ) within the project "Regional Atmospheric Modelling" (Project Id 0302).

Appendix A. Statistical indicators and model performance indicators

In the statistical analysis of the model performance, the following statistical indicators are used: normalized mean bias (NMB), standard deviation (STD), root mean square error (RMSE), correlation coefficient (Corr), index of agreement (IOA) and the fraction of predictions within a factor of two of observations (FAC2). The overall bias captures the average deviations between the model and observed data and the normalized mean bias is given by:

$$NMB = \frac{\overline{M} - \overline{O}}{\overline{O}}, \tag{A1}$$

where M and O stand for the model and observation results, respectively. The overbars indicate the time average over N time intervals (number of observations). The root mean square error combines the magnitudes of the errors in predictions for various times into a single measure and is defined as:

$$RMSE = \sqrt{\frac{1}{N} * \sum_{i=1}^{N} (M_i - O_i)^2}, \tag{A2}$$

where subscript i indicates the time step (time of observation values). RMSE is a measure of accuracy, to compare prediction errors of different models for a particular data and not between datasets, as it is scale-dependent. The correlation coefficient (Pearson r) for the temporal correlation is defined as:

$$r = \frac{\sum_{i=1}^{n} (O_i - \overline{O}) \square (M_i - \overline{M})}{\sqrt{\sum_{i=1}^{n} (O_i - \overline{O})^2 \square \sum_{i=1}^{n} (M - \overline{M})^2}}, \tag{A3}$$

including the standard deviation of model STDM and observation STDO data, respectively. The standard deviations are:

$$STDM = \sqrt{\frac{1}{N-1} * \sum_{i=1}^{N} (M_i - \overline{M})^2} \tag{A4}$$

$$STDO = \sqrt{\frac{1}{N-1} * \sum_{i=1}^{N} (O_i - \overline{O})^2} \tag{A5}$$

The index of agreement is defined as:

$$IOA = 1 - \frac{\sum_{i=1}^{N} (O_i - M_i)^2}{\sum_{i=1}^{N} (|M_i - \overline{M}| + |O_i - \overline{O}|)^2} \tag{A6}$$

An IOA value close to 1 indicates agreement between modelled and observed data. The denominator in Eq. (A6) is referred

To as the potential error. The fraction of modelled values within a factor of two (FAC2) of the observed values are the fraction of model predictions that satisfy is defined as:

$$0.5 \leq \frac{M_i}{O_i} \leq 2.0 \tag{A7}$$

For evaluation of modelled values in rural areas, the acceptance criteria is FAC2 $\geq$ 0.5, while in urban areas it is FAC2 $\geq$ 0.3 (Hanna and Chang, 2012). The indicator H_{perc} for the model capability to reproduce extreme events, e.g. exceedances is defined as:

$$H_{perc} = \frac{|M_{perc} - O_{perc}|}{\beta U_{95}(O_{perc})} \quad and \quad MPC: \; H_{perc} \leq 1 \tag{A8}$$

Where *"perc"* is the selected (high) percentile, M_{perc} and O_{perc} are the modelled and observed values corresponding to the selected percentile (Thunis et al., 2012).

Appendix B. Time series and time variation plots of modelled versus measured concentrations

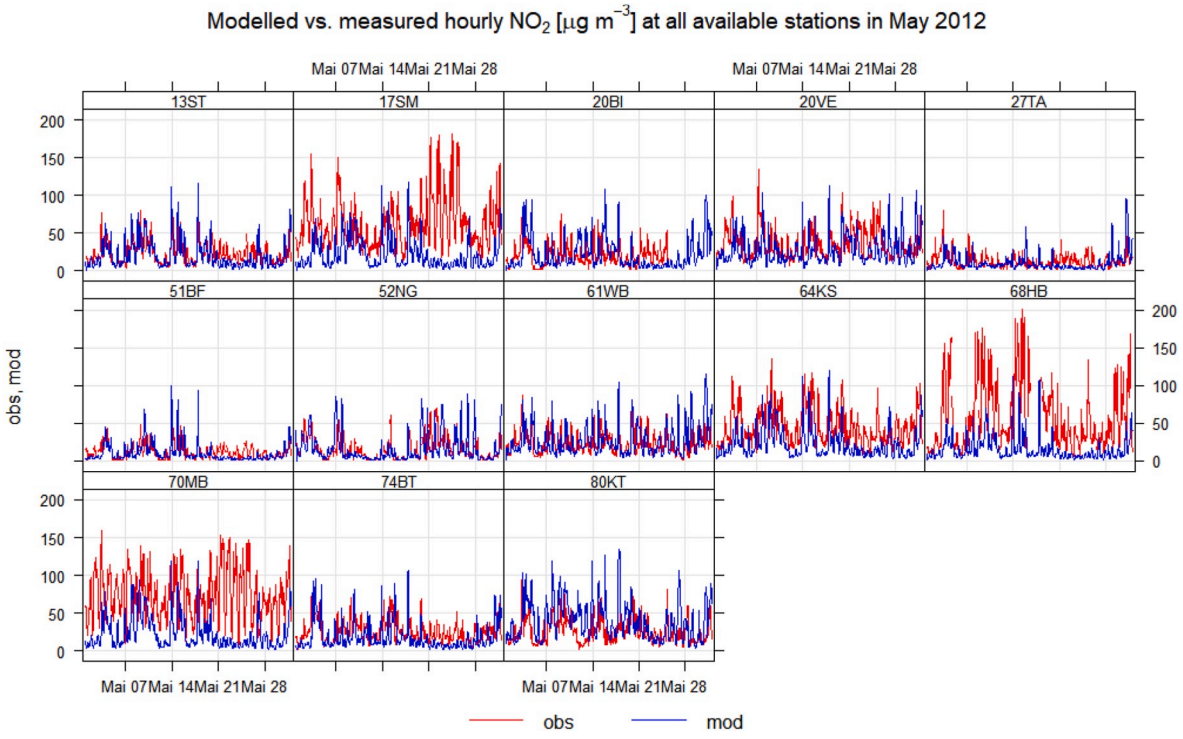

Fig. B1. Modelled vs. measured hourly NO_2 at all available stations in May 2012. The plot is created with the R Openair package and applies all available measurements versus modelled concentrations.

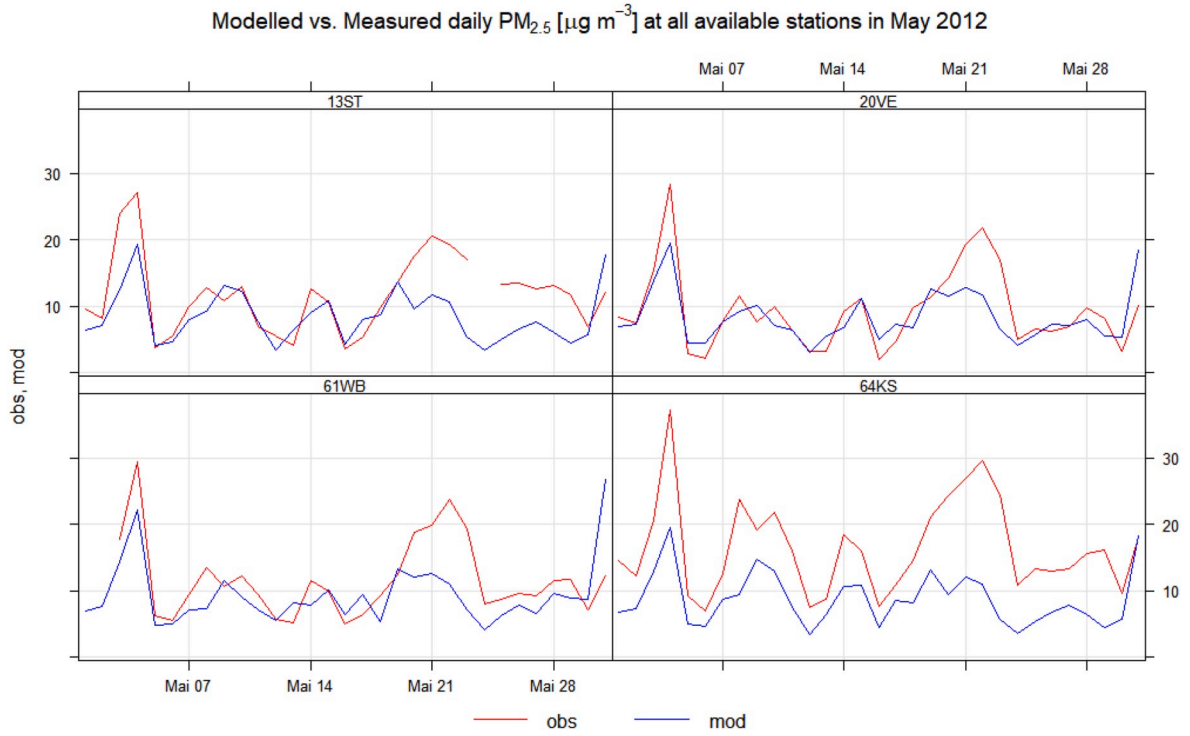

Fig. B2. Modelled vs. measured daily $PM_{2.5}$ at all available stations in May 2012. The plot is created with the R Openair package and applies all available measurements versus modelled concentrations.

Appendix C. Emission reductions in the "land-powered ships" and "inner city zone" scenario, compared to total and shipping/traffic emissions of PM2.5 and NOx

Table C1
Emission reductions in the "land-powered ships" and "inner city zone" scenario, compared to total and shipping / traffic emissions of $PM_{2.5}$ and NO_x.

	[t]	rel. to total emissions	rel. to shipping or traffic emissions	[t]	rel. to total emissions	rel. to shipping or traffic emissions
Total reference emissions	17882	100%	–	2449	100%	–
Scenario "land-powered ships"						
Shipping reference emissions	4902	27.41%	100%	157	6.41%	100%
Avoided emissions at berth in "land-powered ships" scenario	1830	10.23%	37.33%	70	2.86%	44.59%
Shipping emissions in "land-powered scenario" (cruising, manoeuvring)	3072	17.18%	62.67%	87	3.55%	55.41%
Scenario "inner city zone"						
Traffic reference emissions	6882	38.49%	100%	1584	64.67%	100%
Avoided emissions in "inner city zone" scenario	1143	6.39%	16.61%	51	2.08%	3.22%
Traffic emissions in "inner city zone" scenario	5739	32.09%	83.39%	1533	62.60%	96.78%
Scenario "combined"						
Emission reductions in "combined" scenarios	2973	16.63%	–	121	4.94%	–

Appendix D. Relative changes in total exposure due to emission reduction scenarios

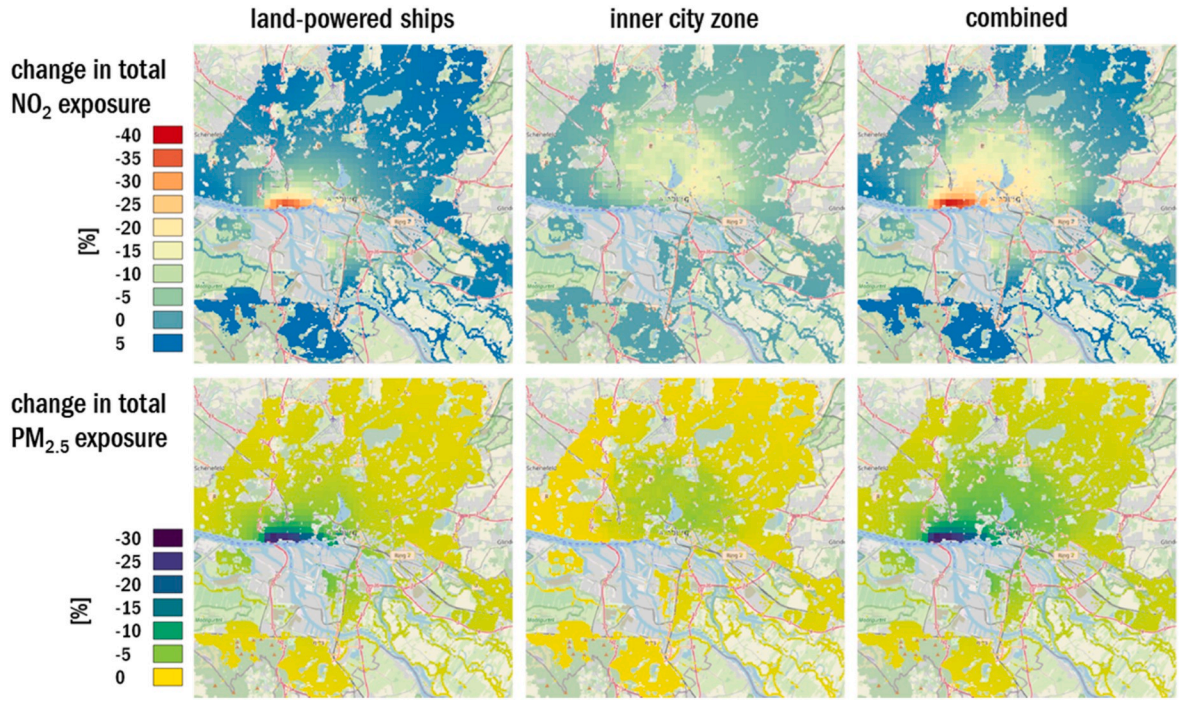

Fig. D1. Modelled relative changes in total NO_2 and $PM_{2.5}$ exposure in the scenarios land-powered ships, inner city zone and combined.

Appendix E. Supplementary data

Supplementary data to this article can be found online at https://doi.org/10.1016/j.atmosenv.2020.117674.

References

Amato, F., Alastuey, A., Karanasiou, A., Lucarelli, F., Nava, S., Calzolai, G., Severi, M., Becagli, S., Gianelle, V.L., Colombi, C., Alves, C., Custódio, D., Nunes, T., Cerqueira, M., Pio, C., Eleftheriadis, K., Diapouli, E., Reche, C., Minguillón, M.C., Manousakas, M.-I., Maggos, T., Vratolis, S., Harrison, R.M., Querol, X., 2016. AIRUSE-LIFE+: a harmonized PM speciation and source apportionment in five southern European cities. Atmos. Chem. Phys. 16, 3289–3309. https://doi.org/10.5194/acp-16-3289-2016.

Ambrey, C.L., Fleming, C.M., Chan, A.Y.-C., 2014. Estimating the cost of air pollution in South East Queensland: an application of the life satisfaction non-market valuation approach. Ecol. Econ. 97, 172–181. https://doi.org/10.1016/j.ecolecon.2013.11.007.

Andersson, C., Bergström, R., Johansson, C., 2009. Population exposure and mortality due to regional background PM in Europe – long-term simulations of source region and shipping contributions. Atmos. Environ. 43, 3614–3620. https://doi.org/10.1016/j.atmosenv.2009.03.040.

Aulinger, A., Matthias, V., Zeretzke, M., Bieser, J., Quante, M., Backes, A., 2016. The impact of shipping emissions on air pollution in the greater North Sea region - Part 1: current emissions and concentrations. Atmos. Chem. Phys. 16, 739–758. https://doi.org/10.5194/acp-16-739-2016.

Azzi, M., Johnson, G.M., Cope, M., 1984. An introduction to the generic reaction set photochemical smog mechanism. In: Proceedings of the 8th International Clean Air Conference. 8th International Clean Air Conference. Melbourne. 6-11 May, Melbourne.

Backes, A.M., Aulinger, A., Bieser, J., Matthias, V., Quante, M., 2016. Ammonia emissions in Europe, part II: how ammonia emission abatement strategies affect secondary aerosols. Atmos. Environ. 126, 153–161. https://doi.org/10.1016/j.atmosenv.2015.11.039.

Batista e Silva, F., Poelman, H., 2016. Mapping Population Density in Functional Urban Areas - A Method to Downscale Population Statistics to Urban Atlas Polygons: JRC Technical Report No. EUR 28194 EN. European Commission Joint Research Centre, Luxembourg.

Beckx, C., Int Panis, L., Arentze, T., Janssens, D., Torfs, R., Broekx, S., Wets, G., 2009. A dynamic activity-based population modelling approach to evaluate exposure to air pollution: methods and application to a Dutch urban area. Environ. Impact Assess. Rev. 29, 179–185. https://doi.org/10.1016/j.eiar.2008.10.001.

Beevers, S.D., Kitwiroon, N., Williams, M.L., Kelly, F.J., Ross Anderson, H., Carslaw, D.C., 2013. Air pollution dispersion models for human exposure predictions in London. J. Expo. Sci. Environ. Epidemiol. 23, 647–653. https://doi.org/10.1038/jes.2013.6.

Behörde für Stadtentwicklung und Umwelt, 2004. Luftreinhalteplan für die Freie und Hanestadt Hamburg. Behörde für Stadtentwicklung und Umwelt. https://www.hamburg.de/contentblob/143556/fb4c0988d6fb0e1738118573d2aa2135/data/luftreinhalteplan-2004.pdf. (Accessed 19 August 2019).

Behörde für Umwelt und Energie, 2017. Luftreinhalteplan für Hamburg (2. Fortschreibung). Behörde für Umwelt und Energie. hamburg.de/contentblob/9024022/7dde37bb04244521442fab91910fa39c/data/d-lrp-2017.pdf. (Accessed 19 August 2019).

Bell, M.L., 2006. The use of ambient air quality modeling to estimate individual and population exposure for human health research: a case study of ozone in the Northern Georgia Region of the United States. Environ. Int. 32, 586–593. https://doi.org/10.1016/j.envint.2006.01.005.

Bieser, J., Ramacher, M.O.P., Prank, M., Solazzo, E., Uppstu, A., 2020. A Multi model study on the impact of emissions on CTMs. In: Mensink, C., Gon, W., Hakam, A. (Eds.), Air Pollution Modeling and its Application XXVI, vol. XXVI. Springer Proceedings in Complexity.

Böhm, J., Wahler, G., 2012. Luftreinhalteplan für Hamburg: 1. Fortschreibung 2012. Behörde für Stadtentwicklung und Umwelt. https://www.hamburg.de/contentblob/3744850/f3984556074bbb1e95201d67d8085d22/data/fortschreibung-luftreinhalteplan.pdf. (Accessed 19 August 2019).

Byun, D., Schere, K.L., 2006. Review of the governing equations, computational algorithms, and other components of the models-3 community multiscale Air quality (CMAQ) modeling system. Appl. Mech. Rev. 59, 51–77. https://doi.org/10.1115/1.2128636.

Carslaw, D.C., Farren, N.J., Vaughan, A.R., Drysdale, W.S., Young, S., Lee, J.D., 2019. The diminishing importance of nitrogen dioxide emissions from road vehicle exhaust. Atmos. Environ. X 1. https://doi.org/10.1016/j.aeaoa.2018.100002.

Carslaw, D.C., Murrells, T.P., Andersson, J., Keenan, M., 2016. Have vehicle emissions of primary NO2 peaked? Faraday Discuss 189, 439–454. https://doi.org/10.1039/c5fd00162e.

Carslaw, D.C., Rhys-Tyler, G., 2013. New insights from comprehensive on-road measurements of NOx, NO2 and NH3 from vehicle emission remote sensing in London, UK. Atmos. Environ. 81, 339–347. https://doi.org/10.1016/j.atmosenv.2013.09.026.

Chen, D., Zhang, Y., Lang, J., Zhou, Y., Li, Y., Guo, X., Wang, W., Liu, B., 2019. Evaluation of different control measures in 2014 to mitigate the impact of ship emissions on air quality in the Pearl River Delta, China. Atmos. Environ. 216, 116911. https://doi.org/10.1016/j.atmosenv.2019.116911.

Copernicus Land Monitoring Service, 2018. Corine land cover. https://land.copernicus.eu/pan-european/corine-land-cover/clc2018.

Corbett, J.J., Koehler, H.W., 2003. Updated emissions from ocean shipping. J. Geophys. Res. 108 https://doi.org/10.1029/2003JD003751.
Corbett, J.J., Winebrake, J.J., Green, E.H., Kasibhatla, P., Eyring, V., Lauer, A., 2007. Mortality from ship emissions: a global assessment. Environ. Sci. Technol. 41, 8512–8518. https://doi.org/10.1021/es071686z.
Denier Van Der Gon, H.A.C., Hendriks, C., Kuenen, J.J.P., Segers, A., Visschedijk, A.J.H., 2011. Description of Current Temporal Emission Patterns and Sensitivity of Predicted AQ for Temporal Emission Patterns: TNO Report. EU FP7 MACC deliverable report D_D-EMIS_1.3, 2011a.
Duque, L., Relvas, H., Silveira, C., Ferreira, J., Monteiro, A., Gama, C., Rafael, S., Freitas, S., Borrego, C., Miranda, A.I., 2016. Evaluating strategies to reduce urban air pollution. Atmos. Environ. 127, 196–204. https://doi.org/10.1016/j.atmosenv.2015.12.043.
EEA, 2017. Digital elevation model over Europe (EU-DEM v1.1). https://www.eea.europa.eu/data-and-maps/data/copernicus-land-monitoring-service-eu-dem. (Accessed 23 January 2019).
Ehrenberger, S., Knitschky, G., Pregger, T., Seum, S., Simon, S., 2020. Land Transport and Energy System Development in Three Integrated Scenarios for Germany – Technology Options, Energy Demand and Emissions. Transportation Research Part D: Transport and Environment (under revision).
European Commission, 2019. Transport in the European union: current trends and issues. https://ec.europa.eu/transport/sites/transport/files/2019-transport-in-the-eu-current-trends-and-issues.pdf. (Accessed 31 August 2019).
Florczyk, A.J., Cobane, C., Ehrlich, D., Freire, S., Kemper, T., Maffeini, L., Melchiorri, M., Pesaresi, M., Politis, P., Schiavina, M., Sabo, F., Zanchettta, L., 2019. GHSL Data Package 2019: JRC Technical Report. EUR 29788 EN, Luxembourg.
Fridell, E., Haeger-Eugensson, M., Moldanova, J., Forsberg, B., Sjöberg, K., 2014. A modelling study of the impact on air quality and health due to the emissions from E85 and petrol fuelled cars in Sweden. Atmos. Environ. 82, 1–8. https://doi.org/10.1016/j.atmosenv.2013.10.002.
Gallego, E., Roca, F.J., Perales, J.F., Guardino, X., Gadea, E., Garrote, P., 2016. Impact of formaldehyde and VOCs from waste treatment plants upon the ambient air nearby an urban area (Spain). Sci. Total Environ. 568, 369–380. https://doi.org/10.1016/j.scitotenv.2016.06.007.
Gately, C.K., Hutyra, L.R., Peterson, S., Sue Wing, I., 2017. Urban emissions hotspots: quantifying vehicle congestion and air pollution using mobile phone GPS data (Barking, Essex : 1987). Environ. Pollut. 229, 496–504. https://doi.org/10.1016/j.envpol.2017.05.091.
Grange, S.K., Lewis, A.C., Moller, S.J., Carslaw, D.C., 2017. Lower vehicular primary emissions of NO2 in Europe than assumed in policy projections. Nat. Geosci. 10, 914–918. https://doi.org/10.1038/s41561-017-0009-0.
Grigoratos, T., Martini, G., 2014. Non-exhaust Traffic Related Emissions - Brake and Tyre Wear PM: Literature Review. European Commission Joint Research Centre. http://publications.jrc.ec.europa.eu/repository/bitstream/JRC89231/jrc89231-online%20final%20version%202.pdf. (Accessed 20 August 2019).
Guerreiro, C., González Ortiz, A., Leeuw, F.d., Viana, M., Colette, A., 2018. Air Quality in Europe - 2018 Report, vol. 1. Publications Office of the European Union, Luxembourg online resource (83.
Hamer, P.D., Walker, S.-E., Sousa-Santos, G., Vogt, M., Vo-Thanh, D., Lopez-Aparicio, S., Ramacher, M.O.P., Karl, M., 2019. The urban dispersion model EPISODE. Part 1: a Eulerian and subgrid-scale air quality model and its application in Nordic winter conditions. Geosci. Model Dev. Discuss. (GMDD) 1–57. https://doi.org/10.5194/gmd-2019-199.
Hamra, G.B., Laden, F., Cohen, A.J., Raaschou-Nielsen, O., Brauer, M., Loomis, D., 2015. Lung cancer and exposure to nitrogen dioxide and traffic: a systematic review and meta-analysis. Environ. Health Perspect. 123, 1107–1112. https://doi.org/10.1289/ehp.1408882.
Hanna, S., Chang, J., 2012. Acceptance criteria for urban dispersion model evaluation. Meteorol. Atmos. Phys. 116, 133–146. https://doi.org/10.1007/s00703-011-0177-1.
Hänninen, O., Knol, A.B., Jantunen, M., Lim, T.-A., Conrad, A., Rappolder, M., Carrer, P., Fanetti, A.-C., Kim, R., Buekers, J., Torfs, R., Iavarone, I., Classen, T., Hornberg, C., Mekel, O.C.L., 2014. Environmental burden of disease in Europe: assessing nine risk factors in six countries. Environ. Health Perspect. 122, 439–446. https://doi.org/10.1289/ehp.1206154.
Hendriks, C., Kranenburg, R., Kuenen, J., van Gijlswijk, R., Wichink Kruit, R., Segers, A., van der Denier Gon, H., Schaap, M., 2013. The origin of ambient particulate matter concentrations in The Netherlands. Atmos. Environ. 69, 289–303. https://doi.org/10.1016/j.atmosenv.2012.12.017.
Heroux, M.E., Braubach, M., Korol, N., Krzyzanowski, M., Paunovic, E., Zastenskaya, I., 2013. The main conclusions about the medical aspects of air pollution: the projects REVIHAAP and HRAPIE WHO/EC. Gigiena i sanitariia 9–14.
Hoek, G., Krishnan, R.M., Beelen, R., Peters, A., Ostro, B., Brunekreef, B., Kaufman, J.D., 2013. Long-term air pollution exposure and cardio- respiratory mortality: a review. Environ. Health : a global access science source 12, 43. https://doi.org/10.1186/1476-069X-12-43.
Hulskotte, J.H.J., Denier Van Der Gon, H.A.C., 2010. Fuel consumption and associated emissions from seagoing ships at berth derived from an on-board survey. Atmos. Environ. 44, 1229–1236. https://doi.org/10.1016/j.atmosenv.2009.10.018.
Hurley, P.J., 2008. TAPM: Technical Description. CSIRO, Aspendale, Vic.
Hurley, P.J., Physick, W.L., Luhar, A.K., 2005. TAPM: a practical approach to prognostic meteorological and air pollution modelling. Environ. Model. Software 20, 737–752. https://doi.org/10.1016/j.envsoft.2004.04.006.
Johnson, G.M., 1984. A simple model for predicting the ozone concentration of ambient air. In: Proceedings of the 8th International Clean Air Conference. 8th International Clean Air Conference. Melbourne. 6-11 May, Melbourne.
Karl, M., Ramacher, M.O.P., 2018. City-scale Chemistry Transport Model EPISODE-CityChem. Zenodo (en).
Karl, M., Walker, S.-E., Solberg, S., Ramacher, M.O.P., 2019. The Eulerian urban dispersion model EPISODE – Part 2: extensions to the source dispersion and photochemistry for EPISODE–CityChem v1.2 and its application to the city of Hamburg. Geosci. Model Dev. (GMD) 12, 3357–3399. https://doi.org/10.5194/gmd-12-3357-2019.
Kiesewetter, G., Amann, M., 2014. Urban PM2.5 Leves under the EU Clean Air Policy Package: TSAP Report #12. International Institute for Applied Systems Analysis. https://ec.europa.eu/environment/air/pdf/TSAP_12.pdf. (Accessed 31 August 2019).
Kotrikla, A.M., Lilas, T., Nikitakos, N., 2017. Abatement of air pollution at an aegean island port utilizing shore side electricity and renewable energy. Mar. Pol. 75, 238–248. https://doi.org/10.1016/j.marpol.2016.01.026.
Kuik, F., Kerschbaumer, A., Lauer, A., Lupascu, A., Schneidemesser, E., von Butler, T.M., 2018. Top–down quantification of NO_x emissions from traffic in an urban area using a high-resolution regional atmospheric chemistry model. Atmos. Chem. Phys. 18, 8203–8225. https://doi.org/10.5194/acp-18-8203-2018.
Künzli, N., Kaiser, R., Medina, S., Studnicka, M., Chanel, O., Filliger, P., Herry, M., Horak, F., Puybonnieux-Texier, V., Quénel, P., Schneider, J., Seethaler, R., Vergnaud, J.-C., Sommer, H., 2000. Public-health impact of outdoor and traffic-related air pollution: a European assessment. Lancet 356, 795–801. https://doi.org/10.1016/S0140-6736(00)02653-2.
Kurtenbach, R., Kleffmann, J., Niedojadlo, A., Wiesen, P., 2012. Primary NO2 emissions and their impact on air quality in traffic environments in Germany. Environ. Sci. Eur. 24, 21. https://doi.org/10.1186/2190-4715-24-21.
Liu, Z., Lu, X., Feng, J., Fan, Q., Zhang, Y., Yang, X., 2017. Influence of ship emissions on urban air quality: a comprehensive study using highly time-resolved online measurements and numerical simulation in shanghai. Environ. Sci. Technol. 51, 202–211. https://doi.org/10.1021/acs.est.6b03834.
Lorentz, H., Düring, I., Schmidt, W., 2010. Berechnung Kfz-bedingter Schadstoffemissionen und Immissionen in Hamburg. Ingenieurbüro Lohmeyer GmbH & Co. KG, Radebeul. https://www.hamburg.de/contentblob/2893032/data/gutachten-lohmeyer.pdf. (Accessed 14 April 2020).
Matthaios, V.N., Triantafyllou, A.G., Albanis, T.A., Sakkas, V., Garas, S., 2018. Performance and evaluation of a coupled prognostic model TAPM over a mountainous complex terrain industrial area. Theor. Appl. Climatol. 132, 885–903. https://doi.org/10.1007/s00704-017-2122-9.
Matthias, V., Arndt, J.A., Aulinger, A., Bieser, J., van der Denier Gon, H., Kranenburg, R., Kuenen, J., Neumann, D., Pouliot, G., Quante, M., 2018. Modeling emissions for three-dimensional atmospheric chemistry transport models, 1995 J. Air Waste Manag. Assoc. 68, 763–800. https://doi.org/10.1080/10962247.2018.1424057.
Matthias, V., Bieser, J., Mocanu, T., Pregger, T., Quante, M., Ramacher, M.O.P., Seum, S., Winkler, C., 2020. Development of a Model System for Road Transport Emissions – Application for Germany. Transportation Research Part D: Transport and Environment (under revision).
Monteiro, A., Durka, P., Flandorfer, C., Georgieva, E., Guerreiro, C., Kushta, J., Malherbe, L., Maiheu, B., Miranda, A.I., Santos, G., Stocker, J., Trimpeneers, E., Tognet, F., Stortini, M., Wesseling, J., Janssen, S., Thunis, P., 2018. Strengths and weaknesses of the FAIRMODE benchmarking methodology for the evaluation of air quality models. Air Qual Atmos Health 11, 373–383. https://doi.org/10.1007/s11869-018-0554-8.
Nawrot, T.S., Perez, L., Künzli, N., Munters, E., Nemery, B., 2011. Public health importance of triggers of myocardial infarction: a comparative risk assessment. Lancet 377, 732–740. https://doi.org/10.1016/S0140-6736(10)62296-9.
Özkaynak, H., Baxter, L.K., Dionisio, K.L., Burke, J., 2013. Air pollution exposure prediction approaches used in air pollution epidemiology studies. J. Expo. Sci. Environ. Epidemiol. 23, 566–572. https://doi.org/10.1038/jes.2013.15.
Pierce, J.R., Theodoritsi, G., Adams, P.J., Pandis, S.N., 2009. Parameterization of the effect of sub-grid scale aerosol dynamics on aerosol number emission rates. J. Aerosol Sci. 40, 385–393. https://doi.org/10.1016/j.jaerosci.2008.11.009.
Pirjola, L., Karl, M., Rönkkö, T., Arnold, F., 2015. Model studies of volatile diesel exhaust particle formation: are organic vapours involved in nucleation and growth? Atmos. Chem. Phys. 15, 10435–10452. https://doi.org/10.5194/acp-15-10435-2015.
Pregger, T., Friedrich, R., 2009. Effective pollutant emission heights for atmospheric transport modelling based on real-world information, 1987 Environmental pollution (Barking, Essex 157, 552–560. https://doi.org/10.1016/j.envpol.2008.09.027.
Rafael, S., Tarelho, L., Monteiro, A., Sá, E., Miranda, A.I., Borrego, C., Lopes, M., 2015. Impact of forest biomass residues to the energy supply chain on regional air quality. Sci. Total Environ. 505, 640–648. https://doi.org/10.1016/j.scitotenv.2014.10.049.
Ramacher, M.O.P., Karl, M., Aulinger, A., Bieser, J., Matthias, V., Quante, M., 2018. The impact of emissions from ships in ports on regional and urban scale air quality. In: Mensink, C., Kallos, G. (Eds.), Air Pollution Modeling and its Application XXV. Springer International Publishing, Imprint, pp. 309–316. Springer, Cham.
Ramacher, M.O.P., Karl, M., Bieser, J., Jalkanen, J.-P., Johansson, L., 2019. Urban population exposure to NO_x emissions from local shipping in three Baltic Sea harbour cities – a generic approach. Atmos. Chem. Phys. Discuss. 1–45. https://doi.org/10.5194/acp-2019-127.
Ramacher, M.O.P., Tang, L., Moldanová, J., Matthias, V., Karl, M., Fridell, E., Johansson, L., 2020. The impact of ship emissions on air quality and human health in the Gothenburg area - Part II: scenarios for 2040. Atmos. Chem. Phys. Discuss. https://doi.org/10.5194/acp-2020-319.
Rasche, M., Walther, M., Schiffner, R., Kroegel, N., Rupprecht, S., Schlattmann, P., Schulze, P.C., Franzke, P., Witte, O.W., Schwab, M., Rakers, F., 2018. Rapid increases in nitrogen oxides are associated with acute myocardial infarction: a case-crossover study. European journal of preventive cardiology 25, 1707–1716. https://doi.org/10.1177/2047487318755804.

Reis, S., Liška, T., Vieno, M., Carnell, E.J., Beck, R., Clemens, T., Dragosits, U., Tomlinson, S.J., Leaver, D., Heal, M.R., 2018. The influence of residential and workday population mobility on exposure to air pollution in the UK. Environ. Int. 121, 803–813. https://doi.org/10.1016/j.envint.2018.10.005.

Requia, W.J., Higgins, C.D., Adams, M.D., Mohamed, M., Koutrakis, P., 2018. The health impacts of weekday traffic: a health risk assessment of PM2.5 emissions during congested periods. Environ. Int. 111, 164–176. https://doi.org/10.1016/j.envint.2017.11.025.

Rockel, B., Will, A., Hense, A., 2008. The regional climate model COSMO-CLM (CCLM). metz 17, 347–348. https://doi.org/10.1127/0941-2948/2008/0309.

Schnabel, P., Beiersdorf, A., 2018. Emission sources and possible mitigation measures of cruise terminals. http://greencruiseport.eu/files/public/download/studies/HPA%20GCP%20report%20Part%20A_Emission%20Sources%20and%20Possible%20Mitigation%20Measures%20of%20Cruise%20Terminals_Final2_26.04.2018.pdf.

Schneider, C., Pelzer, M., Toenges-Schuller, N., Nacken, M., Niederau, A., 2016. ArcGIS basierte Lösung zur detaillierten, deutschlandweiten Verteilung (Gridding) nationaler Emissionsjahreswerte auf Basis des Inventars zur Emissionsberichterstattung: Forschungskennzahl 3712 63 240 2. Texte 71/2016. Umweltbundesamt.

Seinfeld, J.H., Pandis, S.N., 1998. Atmospheric Chemistry and Physics from Air Pollution to Climate Change. Wiley, New York.

Seum, S., Ehrenberge, S., Heinrichs, M., Kuhnimhof, T., Müller, S., Pak, H., Pregger, T., Winkler, C., 2020. Building Three Different Transport Scenarios for Germany until 2040. Transportation Research Part D: Transport and Environment (under revision).

Sillman, S., 1999. The relation between ozone, NOx and hydrocarbons in urban and polluted rural environments. Atmos. Environ. 33, 1821–1845. https://doi.org/10.1016/S1352-2310(98)00345-8.

Simpson, D., Benedictow, A., Berge, H., Bergström, R., Emberson, L.D., Fagerli, H., Flechard, C.R., Hayman, G.D., Gauss, M., Jonson, J.E., Jenkin, M.E., Nyíri, A., Richter, C., Semeena, V.S., Tsyro, S., Tuovinen, J.-P., Valdebenito, Á., Wind, P., 2012. The EMEP MSC-W chemical transport model – technical description. Atmos. Chem. Phys. 12, 7825–7865. https://doi.org/10.5194/acp-12-7825-2012.

Smit, R., Brown, A.L., Chan, Y.C., 2008. Do air pollution emissions and fuel consumption models for roadways include the effects of congestion in the roadway traffic flow? Environ. Model. Software 23, 1262–1270. https://doi.org/10.1016/j.envsoft.2008.03.001.

Soares, J., Kousa, A., Kukkonen, J., Matilainen, L., Kangas, L., Kauhaniemi, M., Riikonen, K., Jalkanen, J.-P., Rasila, T., Hänninen, O., Koskentalo, T., Aarnio, M., Hendriks, C., Karppinen, A., 2014. Refinement of a model for evaluating the population exposure in an urban area. Geosci. Model Dev. (GMD) 7, 1855–1872. https://doi.org/10.5194/gmd-7-1855-2014.

Sofiev, M., Winebrake, J.J., Johansson, L., Carr, E.W., Prank, M., Soares, J., Vira, J., Kouznetsov, R., Jalkanen, J.-P., Corbett, J.J., 2018. Cleaner fuels for ships provide public health benefits with climate tradeoffs. Nat. Commun. 9, 406. https://doi.org/10.1038/s41467-017-02774-9.

Tang, L., Ramacher, M.O.P., Moldanova, J., Matthias, V., Karl, M., Johansson, L., 2020. The impact of ship emissions on air quality and human health in the Gothenburg area – Part 1: current situation. Atmos. Chem. Phys. Discuss. in preparation.

Thunis, P., Pederzoli, A., Pernigotti, D., 2012. Performance criteria to evaluate air quality modeling applications. Atmos. Environ. 59, 476–482. https://doi.org/10.1016/j.atmosenv.2012.05.043.

Timmers, V.R.J.H., Achten, P.A.J., 2018. Non-exhaust PM emissions from battery electric vehicles. In: Amato, F. (Ed.), Non-Exhaust Emissions. Elsevier, pp. 261–287.

Tonnesen, S., Jeffries, H.E., 1994. Inhibition of odd oxygen production in the carbon bond four and generic reaction set mechanisms. Atmos. Environ. 28, 1339–1349. https://doi.org/10.1016/1352-2310(94)90281-X.

UBA, 2010. Handbook of Emission Factors for Road Transport (In German). Umweltbundesamt. https://www.hbefa.net/d/. (Accessed 19 August 2019).

Uherek, E., Halenka, T., Borken-Kleefeld, J., Balkanski, Y., Berntsen, T., Borrego, C., Gauss, M., Hoor, P., Juda-Rezler, K., Lelieveld, J., 2010. Transport impacts on atmosphere and climate: land transport. Atmos. Environ. 44, 4772–4816. https://doi.org/10.1016/j.atmosenv.2010.01.002.

Unger, N., Shindell, D.T., Koch, D.M., Streets, D.G., 2008. Air pollution radiative forcing from specific emissions sectors at 2030. J. Geophys. Res. 113, 955. https://doi.org/10.1029/2007JD008683.

van der Denier Gon, H., Hulskotte, J., Jozwicka, M., Kranenburg, R., Kuenen, J., Visschedijk, A., 2018. European emission inventories and projections for road transport non-exhaust emissions. In: Amato, F. (Ed.), Non-Exhaust Emissions. Elsevier, pp. 101–121.

van der Denier Gon, H.A.C., Bergström, R., Fountoukis, C., Johansson, C., Pandis, S.N., Simpson, D., Visschedijk, A.J.H., 2015. Particulate emissions from residential wood combustion in Europe – revised estimates and an evaluation. Atmos. Chem. Phys. 15, 6503–6519. https://doi.org/10.5194/acp-15-6503-2015.

Walker, S.E., Solberg, S., Denby, B., 2003. Development and Implementation of a Simplified EMEP Photochemistry Scheme for Urban Areas in EPISODE: NILU TR 13/2003. Norwegian Institute for Air Research.

WHO, 2006. Air Quality Guidelines: Global Update 2005. Particulate Matter, Ozone, Nitrogen Dioxide, and Sulfur Dioxide. World Health Organization, Copenhagen, Denmark.

WHO, 2016a. Health risk assessment of air pollution – general principles. http://www.euro.who.int/_data/assets/pdf_file/0006/298482/Health-risk-assessment-air-pollution-General-principles-en.pdf. (Accessed 19 August 2019).

WHO, 2016b. WHO Expert Consultation: Available Evidence for the Future Update of the WHO Global Air Quality Guidelines (AQGs) (Meeting report, Bonn).

Wing, S.E., Bandoli, G., Telesca, D., Su, J.G., Ritz, B., 2018. Chronic exposure to inhaled, traffic-related nitrogen dioxide and a blunted cortisol response in adolescents. Environ. Res. 163, 201–207. https://doi.org/10.1016/j.envres.2018.01.011.

Xu, H., Bechle, M.J., Wang, M., Szpiro, A.A., Vedal, S., Bai, Y., Marshall, J.D., 2019. National PM2.5 and NO2 exposure models for China based on land use regression, satellite measurements, and universal kriging. Sci. Total Environ. 655, 423–433. https://doi.org/10.1016/j.scitotenv.2018.11.125.

Zhang, K.M., Wexler, A.S., Zhu, Y.F., Hinds, W.C., Sioutas, C., 2004. Evolution of particle number distribution near roadways. Part II: the 'Road-to-Ambient' process. Atmos. Environ. 38, 6655–6665. https://doi.org/10.1016/j.atmosenv.2004.06.044.